A peer-reviewed version of this preprint was published in PeerJ on 3 September 2015.

An explanation of the relationships between mass, metabolic rate and characteristic length for placental mammals

Charles C. Frasier

Organizationally unaffiliated in San Diego, California, United States of America

Abstract. The Mass, Metabolism and Length Explanation (MMLE) was advanced in 1984 to explain the relationship between metabolic rate and body mass for birds and mammals. This paper reports on a modernized version of MMLE. MMLE deterministically predicts the absolute value of Basal Metabolic Rate (BMR) and body mass for individual animals. MMLE is thus distinct from other examinations of these topics that use species-averaged data to estimate the parameters in a statistically best fit power law relationship such as BMR = a(body mass)^b. Beginning with the proposition that BMR is proportional to the number of mitochondria in an animal, two primary equations are derived that predict BMR and body mass as functions of an individual animal's characteristic length and sturdiness factor. The characteristic length is a measureable skeletal length associated with an animal's means of propulsion. The sturdiness factor expresses how sturdy or gracile an animal is. Eight other parameters occur in the equations that vary little among animals in the same phylogenetic group. The present paper modernizes MMLE by explicitly treating Froude and Strouhal dynamic similarity of mammals' skeletal musculature, revising the treatment of BMR and using new data to estimate numerical values for the parameters that occur in the equations. A mass and length data set with 575 entries from the orders Rodentia, Chiroptera, Artiodactyla, Carnivora, Perissodactyla and Proboscidae is used. A BMR and mass data set with 436 entries from the orders Rodentia, Chiroptera, Artiodactyla and Carnivora is also used. With the estimated parameter values MMLE can exactly predict every BMR and mass datum from the BMR and mass data set with no error and thus no unexplained variance. Furthermore MMLE can exactly predict every body mass and length datum from the mass and length data set with no error and thus no unexplained variance. Whether or not MMLE can simultaneously exactly predict an individual animal's BMR and body mass given its characteristic length awaits analysis of a data set that simultaneously reports all three of these items for individual animals. However for many of the addressed phylogenetic homogeneous groups, MMLE can predict the exponent obtained by regression analysis of the BMR and mass data using the exponent obtained by regression analysis of the mass and length data. This argues that MMLE may be able to accurately simultaneously predict BMR and mass for an individual animal.

Introduction. Most theoretical treatments of Basal Metabolic Rate (BMR) have focused on the exponent in a relationship of the form $BMR = aW^b$ where W is body mass. Two concepts have dominated. One concept is geometric similarity in which the value of the exponent b = 2/3. The theoretical explanations for this value of the exponent generally involve a balance between heat production and its loss through the body surface (Hulbert & Else, 2004; Clarke, Rothery & Isaac, 2010; Roberts, Lightfoot & Porter, 2010; White, 2010; Roberts, Lightfoot & Porter, 2011; Seymour & White, 2011). In the other concept b = 3/4 (Kleiber, 1932; Kleiber, 1961). This has been known as "Kleiber's Law". A theoretical explanation for b = 3/4 was proposed based on a fractal network for a body's resource supply system (Seymour & White, 2011). More recently theoretical explanations involving resource distribution networks for which the value of the exponent b can be as small as 2/3 or as large as 3/4 have been proposed (Banavar et al. 2010). The metabolic-level boundaries hypothesis proposes that the exponent b is proportional to the proportions of influence of volume and surface area boundary constraints and thus has a value between 2/3 and 1.0 (Glazier, 2010).

More microscopically, it has been proposed that an animal's BMR is proportional to the total number of mitochondria in its tissues (Smith, 1956) or to the sum of the metabolic rates of its constituent cells (Kozlowski, Konarzewski & Gawelczyk, 2003). At an even smaller scale it has been proposed in membrane pacemaker theory (Hulbert & Else, 1999) that BMR is governed by the degree of polyunsaturation of membrane phospholipids or, in the Quantum Metabolism theory (Agutter & Tuszynski, 2011), by molecular-cellular processes.

Recent analyses of BMR, body mass data have argued that there is no single exponent b that applies to a phylogenetic class such as mammals. The relationship is more complicated than $BMR = aW^b$ (Kolokotrones et al, 2010). It has also been argued that there are different exponents for different phylogenetic groups such as mammal orders (White, Blackburn & Seymour, 2009; Capellini, Venditti & Barton, 2010)or different orders among insects, fish, reptiles and birds as well as mammals (Isaac & Carbone, 2010).

The dynamic energy budget (DEB) hypothesis (Sousa et al, 2010; White CR et al, 2011; Maino et al, 2014) can predict the absolute value of BMR rather than the exponent b in the relationship aW^b.

In 1984 the author of the current paper proposed the Mass, Metabolism and Length Explanation (MMLE) theory that also predicts the absolute value of BMR rather than just the exponent b in the relationship $BMR = aW^b$ (Frasier, 1984). A purpose of developing MMLE theory was to relate BMR to measurable skeletal dimensions with the hope of estimating the BMR of extinct animals. Starting with the (Smith, 1956) proposal that an animal's BMR is proportional to the total number of mitochondria in its tissues the theoretical derivation took a course that resulted in equations for predicting the absolute value of body mass as a function of a skeletal length dimension as well as predicting the absolute value of BMR as a function of that skeletal

73 dimension. Used together these equations can predict the absolute value of BMR as a function of
74 body mass. This paper will frequently be referred to as the 'original paper' in the present paper.

75 McNab (McNab, 1988) questioned what should be the best measure of body size against which
76 to scale various functions such as BMR. He presented good reasons why body mass is more
77 variable than linear dimensions in adult mammals. Nevertheless McNab concluded that he would
78 use body mass for want of a better measure of body size. Mass may be an even less reliable
79 measure of body size among bats in which it may vary by as much as 15% to 50% daily (Iriarte-
80 Diaz et al, 2012).

81 The simplest relationship between body mass and a skeletal length dimension would be
82 geometric similarity in which body mass would be proportional to the cube of the length or,
83 equivalently, the length would be proportional to the cube root of the mass. However Galileo, as
84 cited in (Christiansen, 1999; Biewener, 2005), recognized in 1638 that geometric similarity
85 implied that small animals would have to be mechanically overbuilt or large animals would have
86 to operate near the limit of mechanical failure. Elastic similarity was proposed as a theoretical
87 solution to this problem (McMahon, 1973; McMahon, 1975) but its predictions did not agree
88 with data (Alexander et al, 1979; Christiansen, 1999). More recently an explanation based on the
89 need of long bones to resist bending and compressive stress has been proposed (Garcia & da
90 Silva, 2004).

91 It has been recognized that in a relationship relating a skeletal length, l, to body mass raised to an
92 exponent, W^x, the exponent may be different for large terrestrial mammals compared to small
93 terrestrial mammals (Christiansen, 1999; Biewener, 2005). (Campione & Evans, 2013) found
94 that the regression between the total circumference of the humerus and femur to body mass
95 exhibits the strongest relationship with the highest coefficient of determination values; and the
96 lowest mean percent prediction error, standard error of the estimate and Akaike Information
97 Criterion values of all bivariate regression models for extant mammals and reptiles.

98 These theoretical explanations for the relationship between skeletal length dimensions and body
99 mass are based on the stresses the bones and their supporting tissues must accommodate. MMLE
100 theory went in a different direction by examining the rate of energy use in skeletal muscle tissues
101 during activity and the relationship between muscle energy use and energy use by a body's other
102 tissues in the basal metabolic rate state.

103 Since the original publication of MMLE the amount of BMR, body mass data has vastly
104 expanded as has the resources with which to analyze it. So the purpose of this paper is to use
105 these resources to revisit MMLE theory and test its ability to predict the absolute values of BMR
106 and body mass for individual animals with the new data. MMLE theory will also be modified as
107 necessary.

108 The running/walking members of the orders Artiodactyla, Carnivora, Perissodactyla and
109 Proboscidea were addressed in the original paper. The present analysis will add Rodentia and

110   Chiroptera (bats) as well as redo the runners/walkers analysis with new data. Rodentia are a
111   small animal counterbalance to the large runners/walkers and they comprise over 40% of
112   placental mammal species. A comprehensive theory should be able to address flying animals as
113   well as terrestrials and bats comprise another 20% of placental mammal species. Swimming
114   animals should also be addressed but there is too little BMR and body mass data to generate
115   reliable results for the orders Pinnipedia, Cetacea and Sirenia. While not addressing the entirety
116   of the placental mammals, the orders that are addressed do represent over two-thirds of the
117   species.

118   **Summary of MMLE Theory.** This section presents an abbreviated version of MMLE theory as
119   originally formulated (Frasier, 1984) together with some necessary modifications.

120   Nearly all of the energy flux that is measured as basal metabolic rate (BMR) is generated by
121   mitochondria. Although there are other ways to measure it, BMR is most commonly measured
122   by oxygen consumption (Hulbert & Else, 2004). The oxygen is consumed by processes that
123   pump protons across the mitochondrion inner membrane. Heat is produced when some of the
124   protons leak back across the membrane in a controlled fashion as in brown fat or as an
125   uncontrolled basal leak. Otherwise the protons cause the phosphorylation of adenosine
126   diphosphate (ADP) to adenosine triphosphate (ATP) as they return across the inner membrane
127   (Jastroch et al, 2010). ATP is the fuel that powers animal tissues.

128   MMLE strives to predict the absolute value of the BMR of an animal rather than the exponent b
129   or the constant a in the relationship aW^b. It calculates BMR by summing the energy allocation to
130   an animal's tissues. The energy allocated to a tissue type is proportional to the number of
131   mitochondria in the tissue. Thus MMLE tries to count the mitochondria in the tissues that
132   compose an animal and then sum these counts for the entire animal. This approach to calculating
133   an animal's BMR was proposed by (Smith, 1956).

134   MMLE also proposes that mitochondria have a lower limit for the rate of energy release that is
135   experienced by an adult in the thermoneutral zone when inactive and post-absorptive. Basal
136   metabolic rate (BMR) is experienced when an animal's mitochondria are in this state. The lower
137   limit for the rate of energy release by a mitochondrion can be different for different tissue types
138   and different phylogenetic groups.

139   The skeletal muscles, heart, kidneys, liver and brain dominate BMR for vertebrates. These
140   tissues account for 75% to 81% of BMR in the reference man (Müller et al, 2013). The heart,
141   kidneys, liver and brain account for more than 60% of human BMR while accounting for less
142   than 6% of body mass. The sum of the energy consumption by each of the non-skeletal muscle
143   tissues that dominate BMR appears to scale with body mass with the same exponent b in the
144   relationship $BMR = aW^b$ as does BMR for the entire body even though the energy consumption
145   for each separate tissue type may not (Wang et al, 2001).

146 Mitochondria are distributed approximately uniformly throughout a muscle. In the other tissues
147 that dominate BMR the mitochondria are distributed in a relatively thin surface that surrounds
148 material containing few mitochondria. The original paper examines the anatomy of the vertebrate
149 liver in detail to show that it is composed of thin surfaces of hepatic cells richly endowed with
150 mitochondria surrounding endothelial linings, blood, bile and other materials with relatively few
151 mitochondria. For these reasons MMLE theory uses a simplified model of a vertebrate's body
152 consisting of two components: 1) volume active tissues in which mitochondria are approximately
153 uniformly distributed throughout the tissue; and 2) surface active tissues in which mitochondria
154 are concentrated in a surface that surrounds materials that contain few mitochondria.

155   Because the skeletal musculature dominates the volume active tissues from an energy
156 perspective, these tissues were called "skeletal musculature" in the original paper. The surface
157 active tissues that are dominated by the heart, kidneys, liver and brain were called "non-skeletal
158 musculature".

159 It was argued in the original paper that the density of mitochondria in the cells composing the
160 surface active tissues was the maximum possible consistent with the functioning of the cells. The
161 skeletal musculature is sized to support the mechanical loads imposed by activity. The density of
162 mitochondria in the skeletal musculature is sufficient to support the mechanical power
163 requirements of the activity.

164 In the BMR state skeletal muscle mitochondria are only supporting local maintenance functions.
165 Mitochondria in the rest of the body may be operating at a greater output level to support their
166 local maintenance functions, the other components of the non-skeletal muscle tissues and the
167 skeletal muscles. Thus the minimum rate of energy release by a mitochondrion should occur with
168 skeletal muscle mitochondria in the BMR state. MMLE uses this possibility to express the rate of
169 energy release by mitochondria in other tissues in the BMR state and in all tissues in non-BMR
170 activity states as amplification constants multiplying the skeletal muscle mitochondrion rate of
171 energy release in the BMR state.

172 MMLE theory proposed that the minimum rate of energy release by a skeletal muscle
173 mitochondrion in the BMR state can be different for different phylogenetic groups.

174 Mitochondria have different respiration rates in different phylogenetic groups (Else & Hulbert,
175 1981; Else & Hulbert, 1985; Hulbert & Else, 2004; Guderley et al, 2005). Assuming that the
176 BMR state minimum rate of skeletal mitochondrion energy release is genetically determined, a
177 difference between related phylogenetic groups implies mutations affecting mitochondrion
178 performance. Mutations in mitochondria DNA that could affect ATP production were found in
179 all of 41 species of mammals that were examined (da Fonseca et al, 2010). But the situation
180 could be more complex as mitochondrial function plastically responds to change through DNA
181 transcription control, mitochondrial membrane composition and proton leak (Seebacher et al,
182 2010).

183   Because a value for the minimum rate of energy release by a skeletal muscle mitochondrion in
184   the BMR state was not available, it was replaced by a non-dimensional parameter, e, which was
185   named the 'mitochondrion capability quotient'. The parameter e is defined as the minimum rate
186   of energy release by a skeletal muscle mitochondrion in the BMR state for a particular
187   phylogenetic group relative to the minimum rate of energy release by a skeletal muscle
188   mitochondrion in the BMR state for walking/running placental mammals. This definition will be
189   further restricted when walking/running placental mammals are addressed later in the present
190   paper.

191   Although it was not addressed in the original paper, the mitochondrion capability quotient should
192   be, among other things, a function of body temperature.

193   Skeletal muscle mitochondria require the support of the functions powered by the mitochondria
194   in the non-skeletal musculature. MMLE theory considers this to be a constraint in that at levels
195   of muscle activity that can be sustained long term without the accumulation of an oxygen debt,
196   the total power produced by muscle mitochondria is proportional to the total power produced by
197   mitochondria in the non-skeletal musculature. Since the total power produced in a tissue type is
198   (e) X (the number of mitochondria in the tissue) X (the amplification constant appropriate for the
199   tissue and the host animal's activity state), it was concluded the power produced by skeletal
200   muscle mitochondria in the BMR state is also proportional to the power produced by
201   mitochondria in the non-skeletal musculature in the BMR state. Since BMR is the sum of these
202   two power components, BMR is equal to the power produced by mitochondria in the non-
203   skeletal muscle body component multiplied by an appropriate constant.

204   This summary of MMLE theory will use the term 'appropriate constant' for intermediate
205   constants needed to make an intermediate relationship an equality. When the intermediate
206   relationships have been combined into the final MMLE equations the constants occurring in
207   those equations will be given unique symbols. The mathematically rigorous derivations are
208   available in the original paper.

209   For skeletal muscle there are additional constraints. The power generated by mitochondria is
210   also proportional to the mechanical power that a muscle must generate during normal activity.
211   The mechanical power is (the force the muscle bears) X (the distance the muscle
212   extends/contracts) X (the frequency of extension/contraction) where each term is evaluated for
213   the host animal's activity state. The power is also proportional to (e) X (the mass specific density
214   of mitochondria in the muscle) X (the muscle's mass) X (the amplification constant appropriate
215   to the activity state of the animal). By analyzing these constraints with respect to the sliding
216   filament theory of muscle contraction, the MMLE theoretical analysis concluded that they could
217   be simultaneously satisfied if the mass of the skeletal muscles were proportional to BMR divided
218   by the fundamental frequency of muscle activity.

219 The actual frequency at which a muscle operates is a multiple of the fundamental frequency. The
220 multiplier is a function of an animal's activity state.

221 Propulsion was considered to be the primary power consuming activity of skeletal muscles for
222 vertebrates. For animals employing similar dynamics for propulsion, muscle mass can be equated
223 to (an appropriate constant) X (BMR) divided by (the fundamental propulsion frequency). To
224 account for different propulsion dynamics, the fundamental frequency was multiplied by yet
225 another appropriate constant.

226 This was how the original paper recognized that dynamic similarity could be used to scale
227 muscle mass for animals of different sizes. Alexander (Alexander, 2005) addressed dynamic
228 similarity in animals in terms of Froude, Reynolds, and Strouhal similarity. This is a physically
229 more meaningful way to address dynamic similarity. MMLE theory in the present paper is
230 modified to embrace these types of dynamic similarity.

231 In the non-skeletal muscle tissues that dominate BMR, the mitochondria are distributed in a
232 relatively thin surface that surrounds material containing few mitochondria. Recognizing this,
233 MMLE theory describes the mass of the non-skeletal musculature in terms of the total surface
234 area of the energetically active surfaces.

235 Being a surface, the non-skeletal muscle surface can be mathematically described as the square
236 of a length multiplied by an appropriate constant. Any length could be used as long as the
237 constant is adjusted to make the relationship exact. For MMLE theory the selected length is one
238 that is related to propulsion dynamics. This selected length is called the 'characteristic length', l.
239 The proportionality constant includes the 'sturdiness factor', s. s is non-dimensional.

240 It is the expression of the sum of the areas of the metabolically active surfaces of the non-
241 skeletal musculature as proportional to $(sl)^2$ that is the fundamental innovation of MMLE theory.

242 The foregoing considerations were consolidated to express the mass of the non-skeletal
243 musculature equal to $((sl)^2 mG_o/e)^{1/y}$ where mG_o is the final appropriate proportionality constant.
244 G_o has the same value and physical dimensions for all values of y. m is a dimensionality factor
245 that adjusts the physical dimensions of this expression to mass. m is determined by y. m is not an
246 independent variable. The dimensionality factor, m, was not part of the original paper.

247 The mass of the skeletal musculature is equal to $(sl)^2 G_m/kfe$ where f is the fundamental
248 frequency of propulsion, and G_m and k are the final appropriate proportionality constants. Since
249 total body mass, W, is the sum of these two components:

250 $$W = (sl)^2 G_m/kfe + ((sl)^2 mG_o/e)^{1/y} \qquad (1)$$

251 The basal metabolic rate, BMR, is:

252 $$BMR = G_r(sl)^2 \qquad (2)$$

253 where G_r is the final appropriate proportionality constant.

254 After analyzing data for running/walking mammals, rodents and bats a general formulation for
255 the fundamental propulsion frequency appears to be $f = c/l^r$ where c is the appropriate
256 proportionality constant and r is an exponent with a value between 0.5 and 1.0 for species in
257 these mammal orders. Substituting this expression for f in equation (1) yields:

$$W = s^2 \, l^{(2+r)}G_m/kce + ((sl)^2 mG_o/e)^{1/y} \qquad (3)$$

259 Animals that are dynamically similar have similar values for the exponent, r.

260 Surrogate characteristic length and body mass data are available in (Nowak, 1999). It has been
261 entered into Microsoft Excel spread sheets that are available as Supplemental Information Data
262 S1, Data S2 and Data S3. The author of the present paper is unaware of any substantial collection
263 of BMR and characteristic length data. There is substantial BMR and body mass data in (McNab,
264 2008). These data are also available with additional data as a Microsoft Excel spread sheet in the
265 Supplementary Information for (Kolokotrones et al, 2010) at
266 www.nature.com/nature/journal/v464/n7289/suppinfo/nature08920.html which was the source
267 that was used for the present paper. To use this data, equations (1) and (2) can be used together
268 to numerically express BMR as a function of body mass.

269 G_o is defined so that m is dimensionless with a value of 1.0 for geometrically similar non-
270 skeletal musculature for which $y = 2/3$.

271 The equation for skeletal muscle mass includes two final appropriate constants: G_m and k. k is a
272 function of the type of dynamic similarity that applies to the type of propulsion used by an
273 animal. G_m and k were defined so that k is non-dimensional with a value of 1.0 for
274 running/walking placental mammals.

275 The dimensions of the final appropriate constants in equations (1) and (2) are physically straight
276 forward. In the meters kilograms seconds (MKS) system of physical units G_m has the dimensions
277 $(kg/m^2 \, sec)$. G_o has the dimensions $(kg^{2/3}/m^2)$ for $y = 2/3$. m has the dimensions necessary to
278 make the expression for the mass of the non-skeletal musculature in equation (1) have the
279 dimension of mass. G_r has the dimensions $(watts/m^2)$. MMLE avoids the physics challenge of the
280 multiplicative constant a in relationships like aW^b when b varies among different phylogenetic
281 groups as was found in (White, Blackburn & Seymour, 2009; Capellini, Venditti & Barton,
282 2010; Isaac & Carbone, 2010; Hudson, Isaac &, Reuman, 2013).

283 It is a signature feature of MMLE theory that the vertebrate body is represented as a combination
284 of masses instead of a single mass. There are at least two masses: 1) the skeletal musculature
285 which is governed by dynamic similarity and in which the power producing organelles are
286 approximately uniformly distributed; and 2) the non-skeletal musculature in which the power
287 producing organelles are concentrated in surfaces that surround material with few power

288   producing organelles. This binary nature of the vertebrate body can lead to different exponents in
289   the relationship BMR = aW^b for different phylogenetic groups within the same infraclass. As
290   cited in (Hulbert & Else, 2004) Hemmingsen observed in 1960 that a body composed with this
291   sort of binary distribution of power producing organelles could account for values of the
292   exponent b that are different from the geometric similarity value of 2/3.

293   In MMLE theory equations (1) and (2) are exact once numerical values for the parameters have
294   been established. G_m, G_o and G_r are universal constants that should apply to all vertebrates. y and
295   m should have the same value for all animals in a phylogenetic group . k is a constant whose
296   value should be similar for all vertebrates that are dynamically similar. The fundamental
297   propulsion frequency, $f = c/l^r$, should be the same function of the characteristic length, l, for all
298   vertebrates that are dynamically similar. e is a constant whose value should be approximately
299   identical for all vertebrates in the same phylogenetic group with the same body temperature. The
300   characteristic length, l, and the sturdiness factor, s, have unique values for each individual
301   animal.

302   MMLE thusly uses 10 parameters to predict the absolute values of the body mass and BMR of a
303   vertebrate. 10 is only one more than the number of factors that McNab (McNab, 2008) found
304   influenced mammal BMR; and it is less than the over 22 parameters needed to best describe the
305   overall mass and temperature dependence of BMR by the (White, Frappell & Chown, 2012)
306   information-theoretic analysis. While that analysis did include insects, spiders, protists and
307   prokaryotes as well as vertebrates, it and McNab's findings do indicate that needing a large
308   number of parameters to predict the absolute value of a vertebrate's body mass and BMR should
309   not be surprising. Even describing the relationships between BMR and body mass, W, and a
310   skeletal dimension, l, for a collection of animals with the simple relationships BMR = aW^b and
311   W = dl^x requires at least five parameters and as many as six if BMR and length data are not for
312   the same individual animals. Simplicity is not necessarily better than complexity (White,
313   Frappell & Chown, 2012).

314   In the original paper G_m/k, G_o and G_r were considered nearly invariant among vertebrates so that
315   there were only five degrees of freedom for equations (1) and (2).

316   With a body mass and characteristic length data set such as (Nowak, 1999), equation (3) is exact
317   because for every datum a value for the sturdiness factor can be found such that the body mass is
318   exactly computed by the equation using this found sturdiness factor and the characteristic length.
319   With a BMR and body mass data set such as (Kolokotrones et al, 2010), equations (2) and (3) are
320   exact because for every datum a value for the sturdiness factor and a value for the characteristic
321   length can be found such that the BMR is exactly computed by equation (2) and the body mass is
322   exactly computed by equation (3) using the found sturdiness factor value and the found
323   characteristic length value.

324 When the gravitational force dominates the dynamics of animals' movement, two animals are
325 dynamically similar when the ratio of gravitational force to inertial force is the same at
326 corresponding stages of their motions. The animals are Froude similar and they have equal
327 Froude numbers, F, where $F = u^2/gl$ and u is speed, l is the characteristic length and g is the
328 acceleration of gravity (Alexander, 2005). Running/walking mammals are Froude similar
329 (Alexander et al, 1979; Alexander, 2005; Raichlen, Pontzer & Shapiro, 2013).

330 Strouhal similarity obtains when inertial forces are proportional to oscillatory forces. Similarity
331 implies equal Strouhal numbers, St, where $St = fl/u$ and f is the frequency, l is the characteristic
332 length and u is speed. The Strouhal number governs a series of vortex growth and shedding
333 regimes for foils undergoing pitching and heaving motions thereby describing the tail or wing
334 kinematics of swimming or flying animals (Taylor, Nudds & Thomas, 2003).

335 Reynolds similarity obtains when inertial forces are proportional to viscous forces. Similarity
336 implies equal Reynolds numbers, R, where $R = ul\rho/\nu$ and u is speed, l is characteristic length, ρ
337 is fluid density and ν is fluid viscosity (Alexander, 2005). Bats are the only animals examined in
338 the present paper for which viscous drag, and hence Reynolds similarity, might be important. As
339 will be seen when bats are addressed Strouhal similarity does apply to bats. If both Reynolds and
340 Strouhal similarity simultaneously apply, then by solving for speed, u, in the definitions of
341 Reynolds and Strouhal numbers, the frequency, f, is seen to be proportional to the inverse of the
342 characteristic length squared , or $f = R \nu/St \rho l^2$. This sort of dependence of the frequency on the
343 characteristic length was not observed. It should be noted, however, that the characteristic length
344 for viscous drag and that for vortex growth and shedding could be different body dimensions.

345 Two animals are geometrically similar if one can be made identical to the other by multiplying
346 all its linear dimensions by the same factor (Alexander, 2005). Properties of geometric similarity
347 include surface area, S, being proportional to the square of the characteristic length, l^2, and
348 simultaneously volume, V, being proportional to the cube of the characteristic length, l^3. Since
349 mass, W, is proportional to volume, mass is also proportional to l^3. From equation (3) geometric
350 similarity of the skeletal musculature means that the fundamental propulsion frequency exponent
351 r = 1.0. The fundamental frequency constant, c, in equation (3) has the dimension of speed. If the
352 non-skeletal musculature is also geometrically similar with y = 2/3, then the entire animal will be
353 geometrically similar.

354 Froude and Strouhal dynamic similarity are separately compatible with geometric similarity.

355 If both Froude and Strouhal similarity simultaneously apply then equating speed in the
356 definitions of the Froude and Strouhal numbers results with the frequency, f, being proportional
357 to the pendulum frequency, $(g/l)^{0.5}$. Substituting this expression for f in equation (1) shows that
358 mass, W, is not proportional to l^3 and thus geometric similarity does not apply.

359
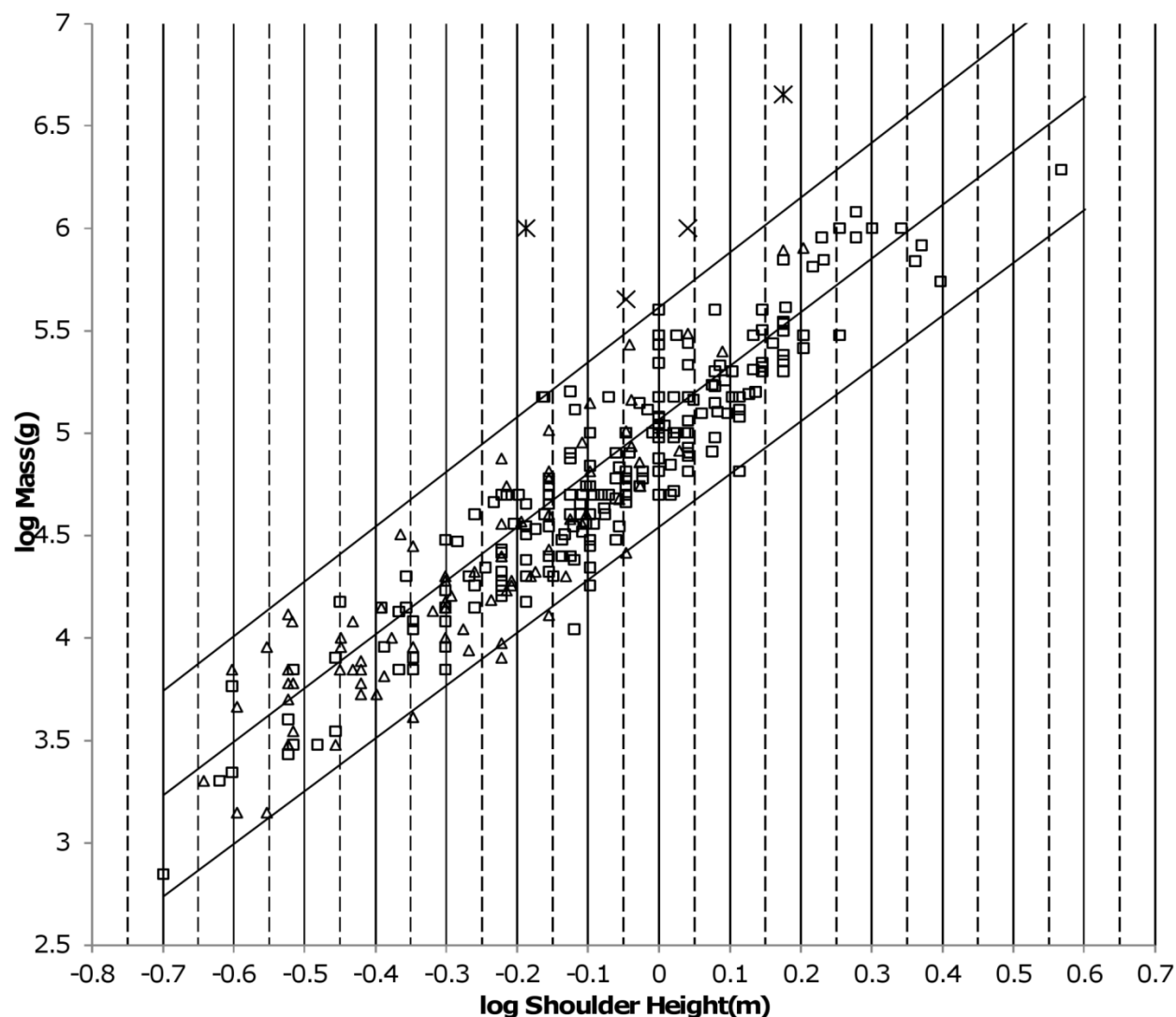
Figure 1. Log body mass as a function of log shoulder height for running/walking Artiodactyla and Carnivora. Data are from (Nowak, 1999). The upper and lower slanted solid lines are MMLE sturdiness factor boundaries for y = 2/3. The upper boundary was generated with a sturdiness factor, s, of the square root of 3, $(3)^{0.5}$. The lower boundary was generated with s = $(3)^{-0.5}$. The middle slanted line was generated with s = 1.0. The slanted lines are for Froude-Strouhal dynamic similarity. The Artiodactyla mass and shoulder height data are marked by open squares. The Carnivora mass and shoulder height data are marked by open triangles. Excluding *Hippopatamus amphibus* marked by crossed Xes and domestic cattle marked by Xes, R_M^2 = 0.9997. The solid vertical lines demark the AVG method first set of cohorts. The dashed vertical lines demark the second set of cohorts.

373 If only one or the other of the dynamic similarities apply without geometric similarity, there is no
374 particular constraint on the fundamental frequency of propulsion, f. Consequently there is no
375 particular constraint on the exponent r in equation (3).

376 From equations (2) and (3) geometric similarity means that BMR is proportional to body mass
377 raised to the 2/3 power, $W^{2/3}$. Simultaneous Froude and Strouhal similarity implies that BMR is
378 proportional to body mass raised to a power greater than 2/3. If only one or the other of the
379 dynamic similarities apply without geometric similarity, BMR could be proportional to body
380 mass raised to a range of powers.

381 Hereafter, when it is stated that geometric similarity applies it also means that either Froude or
382 Strouhal dynamic similarity also applies.

383 Examining body mass and BMR from the skeletal length perspective rather than from the body
384 mass perspective lead to the concept of the sturdiness factor. The sturdiness factor is a most
385 important concept of MMLE theory.

386 The sturdiness factor is best understood by looking at Fig.1. Figure1 plots 314 samples of log
387 body mass versus log shoulder height for running/walking mammals from the orders
388 Artiocactyla and Carnivora obtained from (Nowak, 1999). Shoulder height is a good surrogate
389 for characteristic length for running/walking mammals as will be discussed in a subsequent
390 section. Three slanting lines are also plotted. The middle line plots equation (3) with the
391 sturdiness factor set to 1.0. The upper line plots equation (3) with the sturdiness factor set to the
392 square root of 3, $(3)^{0.5}$. The lower line plots equation (3) with the sturdiness factor set to $(3)^{-0.5}$.
393 Excluding *Hippopatamus amphibus* and domestic cattle, over 97% of the data are contained
394 between the upper and lower slanting lines.

395 The data bordering the upper line are for sturdy animals such as a large American black bear
396 (*Ursus americanus*) with W = 270 kg, l = 0.91 m and s = 1.63 or a large water chevrotain
397 (*Hyemoschus aquaticus*) with W = 15 kg, l = 0.355 m and s = 1.35. The data bordering the lower
398 line is for gracile animals such as a small bob cat (*Felis rufus*) with W = 4.1 kg, l = 0.45 m and s
399 = 0.556 or a large roe deer (*Capreolus pygargus)* with W = 50 kg, l = 1.0 m and s = 0.687. At the
400 same characteristic length an animal with a greater sturdiness factor is more massive than an
401 animal with a lesser sturdiness factor - hence the nomenclature 'sturdiness' factor.

402 The sturdiness factor adds additional information about the physique of an animal that is missing
403 from relationships of the form aW^b. At the same characteristic length, an animal with a greater
404 sturdiness factor has more skeletal muscle and non-skeletal muscle mass and hence more
405 mitochondria. Its BMR should be greater than that of a less sturdy animal as is reflected by
406 equation (2).

407
408

409 **Methods.** Determining numerical values for the universal constants G_m, G_o and G_r requires three
410 equations. Since equation (3) is just a version of equation (1) another equation is required.
411 Numerical values for the constants G_m and G_o could be obtained by solving equation (3) for two
412 different samples of body mass and characteristic length, l. MMLE uses a more general
413 approach.

414 An approximation to equations (1) and (3) is:

$$W = dl^x \tag{4}$$

416 This expression is useful for establishing the approximate relationship between body mass, W,
417 and characteristic length, l, by regression analysis of W, l data for a group of animals. For least
418 squares regression a figure of merit for how well the expression represents the data is the
419 coefficient of determination, R^2. The coefficient of determination measures the fraction of the
420 dependent variable's variance that is explained by the expression.

421 Least squares regression is performed on the logarithmic version of equation (4), $\log(W) = \log(d)$
422 $+ x\log(l)$, to obtain best estimate values for $\log(d)$ and x.

423 Another useful expression is obtained by equating the derivatives with respect to $\log(l)$ of the
424 logarithms of equations (3) and (4) to obtain, for s = 1.0 and geometrically similar non-skeletal
425 musculature where y = 2/3, an equation for the exponent x in equation (4):

$$x = 2.0 + r + (1-r)(G_o/e)^{3/2}/(l^{(r-1)}G_m/kec + (G_o/e)^{3/2}) \tag{5}$$

427 Equation (5) is the third equation needed to establish numerical values for the universal constants
428 G_m, G_o and G_r.

429 The usual way to get the best estimate value for the parameter x in equations like equation (4)
430 has been by regression analysis of the logarithmic version of the equation. The analyses have
431 used species-averages in which a datum is the average value for a collection of individuals from
432 a single species. In ordinary least squares (OLS) and reduced major axis (RMA) regression
433 analyses it has been assumed that the species-averaged data are statistically independent.
434 Phylogenetically informed (PI) analyses assume that the data are not independent but covary
435 with the degree of phylogenetic relatedness between species. These regression methods are
436 reviewed in detail by (White & Kearney, 2014).
437
438 By equations (2) and (3) MMLE deterministically predicts the absolute value of BMR and body
439 mass for individual samples rather than a statistical best fit average value for a collection of
440 individuals from a single species. MMLE is thus compatible with data sets that contain
441 individual animal data. It is also compatible with species-averaged data sets by considering each
442 species-averaged datum to correspond with at least one individual member of the species.
443

444 If a group of animals have nearly identical values for all the parameters occurring in equation (2)
445 and (3) except for characteristic length, l, and sturdiness factor, s, then BMR and body mass can
446 be regressed on characteristic length with sturdiness factor boundaries as illustrated in Fig. 1. As
447 long as the only parameters in equations (2) and (3) that distinguish one individual animal from
448 another are characteristic length and sturdiness factor the individuals included in the analysis
449 may be from different species, genera, families, and even orders. Such a group of animals are
450 called a MMLE phylogenetic homogeneous group herein.

451

452 The AVG regression method exploits this feature of MMLE to use individual animal data such
453 as the unmodified data from (Nowak, 1999). The AVG regression method is unique to MMLE.
454 A detailed explanation of the method is given in (Article S1).

455 The appendix to the original paper shows that the OLS regression relationship between body
456 mass and characteristic length is given by the equivalent of equation (3) evaluated with a
457 sturdiness factor value of s = 1.0 for a MMLE phylogenetic homogeneous group. The s = 1.0
458 regression relationship is plotted by the middle slanting line in Fig. 1. For any particular
459 characteristic length, the mean of the logs of all body masses with that characteristic length that
460 are uniformly distributed between the upper and lower sturdiness factor boundaries is the log of
461 the body mass predicted by equation (3) evaluated with a sturdiness factor of s = 1.0. Using the
462 AVG regression method, MMLE takes advantage of this property to get linear regression
463 relationships between log body mass regressed on log characteristic length with coefficients of
464 determination, R^2, that are very nearly 1.0.

465 The next section describes using the AVG regression method on characteristic length, body mass
466 data for running/walking placental mammals in the families Artiodactyla and Carnivora from
467 (Nowak, 1999) to estimate numerical values for the parameter x in equations (4) and (5) and then
468 the parameters G_m/k and G_o in equations (1) and (3). The numerical values for G_m/k and G_o apply
469 to all placental mammals.

470 BMR and characteristic length data to estimate a numerical value for the parameter G_r in
471 equation (2) was unavailable. Species-averaged BMR and body mass data was available from
472 (Kolokotrones et al, 2010).

473 By equations (2) and (4),

$$BMR = G_r(W/d)^{2/x} \qquad\qquad (6)$$

475 Since d and x are estimated by regression analysis this expression is reliable only if the
476 coefficient of determination, R^2, is nearly unity for the analysis that estimated d and x. From
477 table 1 in the next section $R^2 = 0.9932$ for the AVG regression analysis that estimated d and x for
478 running/walking placental mammals in the families Artiodactyla and Carnivora. Although there
479 are complications that will be discussed in the next section a reasonable estimate for the
480 numerical value of G_r is obtained.

481 To solve for a numerical value of G_r an allometric expression of the form $BMR = aW^b$ is
482 obtained by regression analysis. If equation (6) is reliable then $b = 2/x$ and $a = G_r/d^{2/x}$.

483 Phylogenetically Informed (PI) Generalized Least Squares regression was used to obtain the
484 needed $BMR = aW^b$ expression. The PI Generalized Least Squares regression analyses were
485 conducted using the BayesTraits computer program (Pagel, Meade & Barker, 2004). PI methods
486 are used to control for an assumed lack of statistical independence among species (Freckleton,
487 Harvey & Pagel, 2002; White & Kearney, 2014).

488 The Microsoft Windows version of BayesTraits together with the companion programs
489 BayesTrees and BayesTreesConverter available at www.evolution.rdg.ac.uk were used. For
490 Rodentia and bats the all mammals phylogenetic tree that is available as supplemental
491 information from the online version of (Fritz, Bininda-Emonds & Purvis, 2009) at
492 http://onlinelibrary.wiley.com/doi/10.111/j.1461-0248.2009.01307.x.suppinfo was used. For
493 running/walking mammals the updated tree for Carnivora that is available from the online
494 version of (Nyakatura & Bininda-Emonds, 2013) at
495 www.ncbi.nlm.nih.gov/pmc/articles/PMC3307490/ was grafted onto the all mammals tree. The
496 analyses were performed with the continuous regression model and maximum likelihood
497 analysis type. The inputs were set to estimate the parameter lambda (see Article S1).

498 Lambda is found by maximum likelihood. It usually varies between 0.0 and 1.0. It is a multiplier
499 of the off-diagonal elements of the Generalized Least Squares variance-covariance matrix.
500 Lambda = 0.0 indicates evolution of traits that is independent of phylogeny, while lambda = 1.0
501 indicates that traits are evolving according to Brownian motion. Intermediate values indicate that
502 traits have evolved according to a process in which the effect of phylogeny is weaker than in the
503 Brownian model (Pagel, 1999; Freckleton, Harvey & Pagel, 2002; Pagel, Meade & Barker, 2004;
504 Capellini, Venditti & Barton, 2010). BayesTraits results generated with lambda = 0.0 are the
505 same as those obtained with Ordinary Least Squares (OLS) linear regression. Results generated
506 with lambda = 1.0 are the same as those generated by phylogenetically independent contrasts
507 (Capellini, Venditti & Barton, 2010). Occasionally lambda was estimated to be greater than 1.0.
508 This can be interpreted as traits that are more similar than what is predicted by Brownian motion
509 (Freckleton, Harvey & Pagel, 2002).

510 Since BayesTraits estimates maximum likelihood for a hypothesis (such as the applicable value
511 of lambda), the log likelihood ratio for two hypotheses can be computed. By convention a value
512 of 4.0 or greater for the ratio is taken as evidence that one of the hypotheses explains the data
513 significantly better than the other (Pagel, 1999).

514 PI regression analyses were performed for both BMR regressed on body mass and body mass
515 regressed on characteristic length. The species-averaged BMR, body mass data from
516 (Kolokotrones et al, 2010) was inputted directly to BayesTraits. The body mass, characteristic
517 length data from (Nowak, 1999) are mostly maximum and minimum measurements of

518 individuals from the same species or genera in which a datum is the measurements for the largest
519 or smallest individual measured in the taxon. Body mass, characteristic length data were taxon-
520 averaged before being inputted to BayesTraits.

521 Together with the dynamic similarity implied by the mode of locomotion for a group of animals,
522 PI regression relationships are helpful for partitioning populations into MMLE phylogenetic
523 homogeneous groups to which the AVG regression technique can be applied as when a
524 geometrically similar partition can be identified by a log(mass) regressed on log(length) slope of
525 3.0 or a log(BMR) regressed on log(mass) slope of 2/3. Since the only parameters in equation (3)
526 that differ between individual members of a MMLE phylogenetic homogeneous group are the
527 characteristic length, l, and the sturdiness factor, s, further consideration of the relatedness of
528 members should not be necessary.

529 Regression analysis measures the error for a datum as the distance between the datum and a line
530 established by the regression analysis. The line minimizes the sum of the squares of the errors.
531 Using Fig. 1 as an example, the usual way of measuring error for a datum is the vertical distance
532 from the datum to the middle slanting line given by equation (3) evaluated with a sturdiness
533 factor s = 1.0. The coefficient of determination, R^2, equals 1.0 − (sum of the squares of the
534 errors)/(variance of the dependent variable). R^2 is interpreted as the fraction of the dependent
535 variable variance that is explained by the regression line (Edwards, 1984). The dependent
536 variable in Fig. 1 is body mass.

537 In MMLE theory the OLS regression line can be replaced by a 'band'. The band is the area
538 enclosed by the sturdiness factor boundaries. Recognizing this fact, R^2 can be replaced by an
539 MMLE version that is denoted "R_M^2". R_M^2 is computed in the same ways as R^2 except that the
540 'error' for a datum that falls between the sturdiness factor boundaries is zero and the 'error' for a
541 datum that that falls outside the sturdiness factor boundaries is the distance between the datum
542 and the nearest sturdiness factor boundary. $R_M^2 = 0.9997$ for the data in Fig. 1.

543 R_M^2 is very nearly unity because the data considered in the present paper mostly lie between the
544 sturdiness factor boundaries or very near to a boundary. Coverage, R, which is the fraction of the
545 data that lies between the boundaries, is another figure of merit that is usually smaller than R_M^2.

546 Equation (3) evaluated with correct sturdiness factors exactly predicts every datum obtained
547 from (Nowak, 1999) that is shown in Fig. 1. There is no error and thus no unexplained variance.
548 R_M^2 is interpreted as a measure of how well data clusters within the sturdiness factor boundaries.
549 R_M^2 is useful for estimating values for the parameters that appear in equation (3) when they may
550 differ from the values established for running/walking placental mammals.

551 By examining individual animal metabolic rates and masses, (Hudson, Isaac &, Reuman, 2013)
552 recently reported substantial metabolic rate heterogeneity at the species level and commented
553 that this is a fact that cannot be revealed by species-averaged data sets. It was further commented
554 that individual data might be more important than species-averaged data in determining the

555 outcome of ecological interactions and hence selection. Heterogeneity is predicted by equations
556 (2) and (3) due to variation of characteristic length and sturdiness factor among the individuals
557 composing a species. The AVG regression method is compatible with species level
558 heterogeneity.

559 Sturdiness factor boundaries and R_M^2 can also apply to the BMR, body mass data from
560 (Kolokotrones et al, 2010). The boundaries are calculated by using equation (3) with the
561 bounding sturdiness factors to calculate the body mass and using equation (2) with the bounding
562 sturdiness factors to calculate the BMR for characteristic lengths that span the range of interest.
563 The associated value of R_M^2 can then computed using the BMR as a function of body mass
564 boundaries.

565 Equations (2) and (3) evaluated with a correct sturdiness factor and characteristic length exactly
566 predicts every BMR and body mass datum used in the present paper that was obtained from
567 (Kolokotrones et al, 2010). There is no error and thus no unexplained variance.

568 As will be discussed later the ability of equation (3) to exactly predict every datum extracted
569 from one data set and its ability, when combined with equation (2), to exactly predict every
570 datum extracted from another data set does not necessarily mean that there is no unexplained
571 variance with MMLE theory.

572 The calculated numerical values reported in the present paper are given with four significant
573 digits to the right of the decimal point. It is suspected that the data used is not accurate enough to
574 support this precision.

575 **Running/Walking Placental Mammals.** This is an abbreviated version of the analysis of
576 running/walking placental mammals. The detailed analysis is available in Supplemental
577 Information Methods Details (Article S1).

578 The original paper established the numerical values for the constants in the MMLE equations by
579 AVG analysis of 163 samples of the running/walking members of the orders Artiodactyla,
580 Carnivora, Perrisodactyla and Proboscidae from (Walker, 1968). The fundamental frequency of
581 propulsion was established as the pendulum frequency obtained when both Froude and Strouhal
582 dynamic similarity apply simultaneously. Limb length was considered to be the characteristic
583 length but little limb length data was available. Shoulder height data was more available, so
584 shoulder height was adopted as an approximation of the characteristic length, l. The results were
585 x = 2.66, G_m/k = 295000 g/m^2 sec and G_o = 1353 g$^{0.667}$/m^2 in the units used in the present paper.
586 By examining the graph of body mass as a function shoulder height for the 163 samples, it was
587 estimated that mass as a function of shoulder height lines computed from equation (3) with
588 sturdiness factor values of the square root of 3, $(3)^{0.5}$, and its inverse, $(3)^{-0.5}$, approximately
589 bounded the data.

590   BMR was predicted to scale as body mass raised to the 2/x power. Since x = 2.66 this meant that
591   BMR scaled as body mass raised to the 0.75 power in agreement with Kleiber's law. Kleiber's
592   law with additional data from (Economos, 1982) was used to estimate the constant G_r in equation
593   (2) to be 142 watts/m^2.

594   An expanded version of the methodology in the original paper was used to determine the
595   constants in equations (1), (2) and (3) in the present paper. AVG and PI regressions of the new
596   body mass on shoulder height data were used to determine the exponent in equation (4). This
597   regression relationship was then to be used to determined body mass at a 'middle' shoulder
598   height. Then equations (3) and (5) were solved simultaneously for the constants G_m/k and G_o
599   occurring in the equations using unity sturdiness factor and unity mitochondrion capability
600   quotient. The method for determining the constant G_r in equation (2) was more complicated.

601   Although (Raichlen, Pontzer & Shapiro, 2013) find that hip joint to limb center of mass is a
602   better length for establishing the pendulum frequency, shoulder height was again used as an
603   approximation of the characteristic length due to its greater availability.

604   226 individual and 129 species-averaged mass and shoulder height samples were obtained from
605   (Nowak, 1999) for Artiodactyla (Data S1). *Hippopotamus amphibius* and *Bos Taurus* (aurochs
606   and domestic cattle) were excluded from the analysis.

607   84 individual and 43 species-averaged mass and shoulder height samples were obtained from
608   (Nowak, 1999) for Carnivora (Data S1). The Mustelidae were mostly excluded because shoulder
609   height was not given except for wolverines (*Gulo gulo*) and honey badgers (*Mellivoracapensis*).
610   Shoulder height was not given for most of the smaller Carnivora so that the smallest sample was
611   a raccoon (*Procyon*) with a mass of 2000g and a shoulder height of 0.228m.

612   Table 1 shows the AVG and PI regression analysis results obtained with this data. From the
613   Artiodactyla + Carnivora AVG mass on shoulder height regression the exponent, x, for equation
614   (4) is 2.61.Since total body mass scales with an exponent, 2.61, that is greater than the exponent
615   with which the skeletal muscle mass scales, 2.5, the non-skeletal muscle mass must scale with an
616   exponent greater than 2.61. The simplest assumption is geometric similarity so that the non-
617   skeletal muscle mass scales with an exponent of 3.0. The corresponding value for y is 2/3.
618   Simultaneously solving equations (4) and (5) results in $G_m/k = 274000$ g/m^2 sec and $G_o = 900$
619   g$^{0.667}$/m^2.

620   The PI mass on shoulder height regression slope for Artiodactyla + Carnivora is not significantly
621   different from 2.5 as the log likelihood ratio for the table 1 slope and 2.5 is less than 4.0. Since
622   for Froude-Strouhal similarity the skeletal musculature scales with an exponent of 2.5, this
623   implies that the non-skeletal musculature also scales with an exponent of 2.5 which means that y
624   = 0.8 in equation (3). The equivalent of equation (5) with y = 0.8 and r = 0.5 only states that x =
625   2.5 and provides no information for estimating G_m/k and G_o. Additionally equation (3) must be
626   used to estimate the dimensionality factor, m.

627

628 G_m/k should not change if y changes. Using the previously established values of G_m/k and G_o

629 with y = 0.8 in equation (3) results with a value for the dimensionality factor of m = 4.425 $g^{0.133}$.

630 _____

631

632 **Table 1.** Results of regression analyses for running/walking placental mammals.

Order or Family	Regression Type	Independent Variable	Dependent Variable	Slope	Intercept	R^2	Number Samples
Artiodactyla + Carnivora	AVG	Height(m)	Mass(g)	2.6112	5.0584	0.9932	NA
	PI(0.89)	Height(m)	Mass(g)	2.4893	5.076	0.8435	172
All	AVG	Height(m)	Mass(g)	2.8711	5.1677	0.9886	NA
	PI(0.92)	Height(m)	Mass(g)	2.4875	5.2517	0.8424	189
Ruminant Artiodactyla	PI(0.0)	Mass(g)	BMR(watts)	0.7805	-1.8058	0.9742	19
Carnivora	PI((0.87)	Mass(g)	BMR(watts)	0.7579	-1.8826	0.909	59
Carnivora less Mustelidae	PI(0.61)	Mass(g)	BMR(watts)	0.758	-1.8937	0.9053	46
Mustelidae less Enhydra	PI(1.0)	Mass(g)	BMR(watts)	0.6852	-1.4688	0.9653	12
Perrisodactyla+Proboscidae	AVG*	Height(m)	Mass(g)	2.26	5.54	0.93	NA
	AVG**	Height(m)	Mass(g)	2.59	5.44	0.96	NA
	PI(1.02)	Height(m)	Mass(g)	1.376	5.716	0.9442	17

633 The regression expressions are: Log(dependent variable) = slope X log(independent variable) +

634 intercept. AVG means the cohort averaging regression method. PI(n) means the phylogenetic

635 informed regression method using BayesTraits and the number in parentheses is the estimated

636 value of lambda. "All" in the Order or Family column means the combination of Artiodactyla,

637 Carnivora, Perissodactyla and Proboscidae. Height(m) is shoulder height in meters. Mass(g) is

638 body mass in grams. BMR(watts) is basal metabolic rate in watts. NA means Not Applicable. *,

639 AVG method first set of cohorts values; **, AVG method second set of cohorts values.

640 _____

641 The new values for G_m/k and G_o are less than the values computed in the original paper. The 163

642 samples in the original paper included two Probicidae and 11 Perissodactyla whereas the 310

643 samples in the present paper were entirely Artiodactyla or Carnivora.

644 Figure 2 shows the MMLE mass as a function of shoulder height sturdiness factor boundaries for

645 simultaneous Froude-Strouhal dynamic similarity as predicted by equation (3) evaluated with the

646 new values for G_m/k and G_o for both y = 2/3 and for y = 0.8. The reference (Nowak, 1999) mass

647 and shoulder height samples for Artiodactyla and Carnivora are also shown. The data spans this

648 full range of sturdiness factor for both values of y. The boundaries are hardly distinguishable for

649 the two y values.

650

651
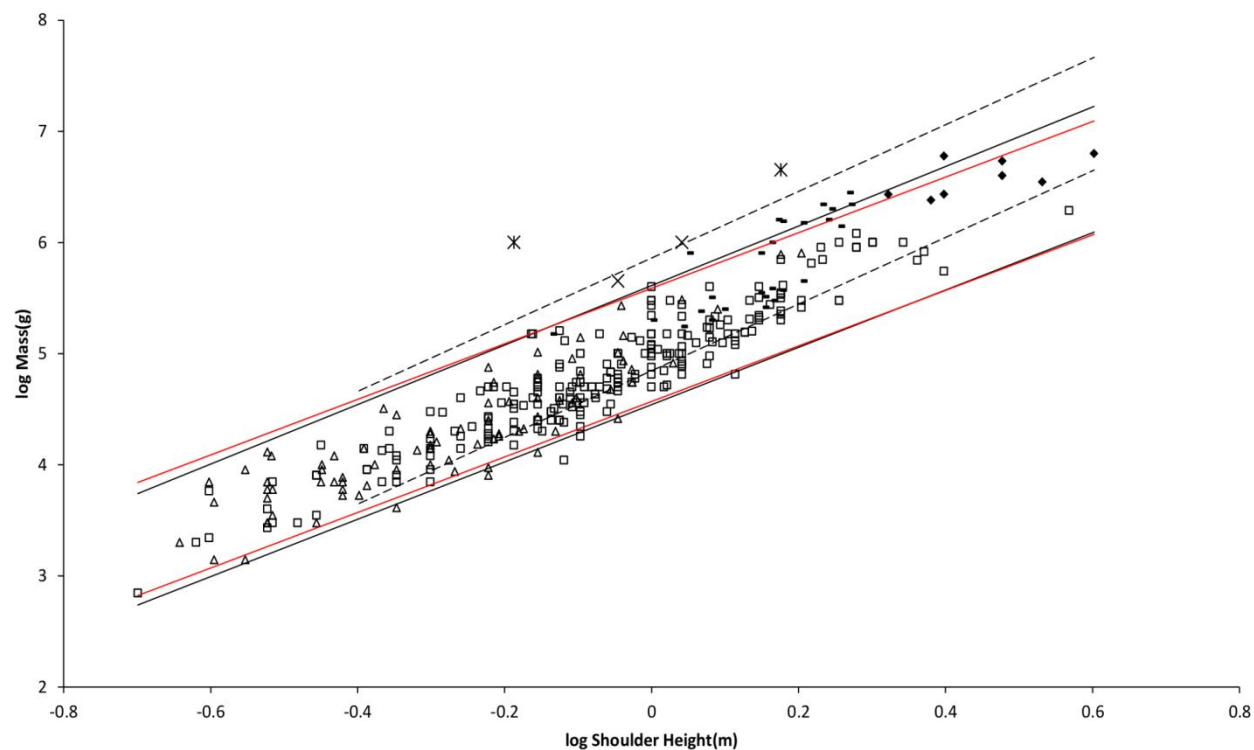
Figure 2. Log body mass as a function of log shoulder height for running/walking placental mammals. Data are from (Nowak, 1999). The solid and dashed lines are MMLE sturdiness factor boundaries. The upper boundaries were generated with a sturdiness factor $s = (3)^{0.5}$. The lower boundaries were generated with $s = (3)^{-0.5}$. The solid boundary lines are for Froude-Strouhal dynamic similarity. The black solid lines are for $y = 2/3$. The colored solid lines are for $y = 0.8$. The dashed boundary lines are for geometric similarity. The colored boundary lines, the geometric similarity boundary lines and the Perissodactyla and Proboscidae mass, shoulder height data have been added to the Artiodactyla and Carnivora data displayed in figure 1. For Artiodactyla and Carnivora $R_M^2 = 0.9997$ with respect to the solid black boundaries and $R_M^2 = 0.9992$ with respect to the colored boundaries. For Perissodactyla and Proboscidae $R_M^2 = 1.0$ with respect to the geometric similarity boundaries. Perissodactyla data are marked with solid rectangles. Proboscidea data are marked with solid diamonds. Aritiodactyla data are marked with open squares. Carnivora data are marked with open triangles. Crossed Xes mark *Hippopotamus amphibious*. Xes mark domestic cattle.

670 26 individual and 14 species-averaged mass and shoulder height samples were obtained from
671 (Nowak, 1999) for Perissodactyla. Eight individual and three species-averaged samples were
672 obtained for Proboscidae (Data S1). Table 1 shows the AVG and PI regression analysis results
673 obtained with this data. The first set of cohorts and the second set of cohorts regression
674 relationships for Perissodactyla and Proboscidae combined differed enough to make the AVG
675 analysis suspect. The slope of the PI relationship is very different from the other relationships'
676 slopes. Upon further analysis the relationship between mass and shoulder height for
677 Perissodactyla and Proboscidae may be better explained by geometric similarity with a
678 fundamental frequency of 1.4 m/sec divided by shoulder height (see Supplemental Information
679 Methods Details (Article S1)).

680 For running/walking placental mammals the reference (Kolokotrones et al, 2010) BMR and body
681 mass species-averaged data set contained 20 samples for Artiodactyla and 58 samples for
682 Carnivora.

683 There are doubts that ruminant Artiodactyla can meet the criteria for measuring BMR (McNab,
684 1997; White & Seymour, 2003). All but one of the Artiodactyla samples were ruminants. For
685 these reasons the BMR and mass data for ruminant Artiodactyla and Carnivora were analyzed
686 separately. Ruminants inability to achieve a post absorptive state should not affect the
687 relationship between body mass and shoulder height so revisiting that analysis because of this
688 issue is not needed.

689 There is a major composition difference between the mass and shoulder height data and the
690 BMR and mass data for Carnivora. Mustelidae compose only about 1% of the mass and shoulder
691 height data whereas they compose over 20% of the BMR and mass data. For this reason the
692 Mustelidae data was separated from the rest of the Carnivora data as shown in table 1.

693 Since the coefficient of determination, R^2, for the AVG Artiodactyla + Carnivora mass on
694 shoulder height regression in table 1 is very nearly unity, equation (6) can be used. With the
695 G_m/k and G_o values just determined, $G_r = 95.6W^{-0.0079}$ watts/m^2. The mass residual is not
696 significant as the log likelihood ratio for the exponent obtained with equation (6) and the
697 exponent in Table 1 is essentially 0.
698
699 Using the Carnivora less Mustelidae PI mass regressed on length and the PI BMR regressed on
700 mass relationships in table 1 results with $G_r = 94.5$ watts/m^2.
701
702 A middle value of $G_r = 95$ watts/m^2 was used to generate the MMLE sturdiness factor boundaries
703 in Fig. 3. As discussed in the summary of the derivation of the MMLE equations, this value of G_r
704 should be the basic value for all non-ruminant placental mammals.

705 Similarly, values for G_{rR} for ruminant Artiodactyla of 138 watts/m^2 and 144 watts/m^2 are
706 obtained. G_{rR} = 138 watts/m^2 was used to generate the MMLE sturdiness factor boundaries in
707 Fig. 3.

708 The difference between the ruminant Artiodactyla and Carnivora less Mustelidae BMR regressed
709 on mass slopes in Table 1 are not significant as the log likelihood ratio is 2.8. However the
710 difference between the intercepts is significant as the log likelihood ratio is greater than 4.0. The
711 significantly different intercepts support separating ruminant Artiodactyla and Carnivora less
712 Mustelidae for BMR analyses.

713

714 An increased mitochondrion capability quotient is not the reason that G_{rR} is greater than G_r. By
715 equation (3) a greater mitochondrion capability quotient would result in a less massive animal for
716 the same characteristic length. Figure 2 shows that both Artiodactyla and Carnivora have similar
717 masses at the same characteristic length. The difference between G_{rR} and G_r is more likely the
718 result of sustained digestive activity by ruminant Artiodactyla (McNab, 1997; White & Seymour,
719 2003).

720 Figure 3 shows the MMLE BMR as a function of body mass sturdiness factor boundaries for
721 Froude-Strouhal similarity evaluated with the new values for G_r and G_{rR}. The boundaries were
722 generated by simultaneously using equations (2) and (3). The differences between the y = 2/3
723 and y = 0.8 curves are due to the different masses predicted by equation (3) for the same
724 characteristic length with the different values of y. The difference between the slopes for the two
725 values of y is significant as the log likelihood ratio is 5.9. In terms of R_M^2 the differences are
726 barely distinguishable.

727 Ruminant Artiodactyla do have a BMR that is elevated with respect to Carnivora of the same
728 mass. The single non-ruminant Artiodactyla datum, a dromedary camel (*Camelus dromedaries*),
729 is embraced by the non-Mustelidae Carnivora MMLE boundaries rather than the ruminant
730 boundaries. The data more than spans the full range of sturdiness factor.

731 Also shown in Fig. 3 is the Mustelidae BMR and mass data. It is better embraced by the
732 ruminant MMLE sturdiness factor boundaries, but Mustidae do not have the digestive features
733 that are the probable source of the ruminants' elevated BMR. The non-Mustelidae Carnivora
734 value for G_r should apply to the Mustelidae also, but their MMLE boundaries hardly embrace
735 any of the Mustelidae data. Sturdiness factor and characteristic length values could be found so
736 that equations (2) and (3) would exactly predict each Mustelidae BMR and mass datum shown in
737 Fig. 3, but the sturdiness factors would mostly be greater than the maximum needed to predict
738 the BMR and mass for other Carnivore families. Other MMLE parameters can be adjusted so
739 that the Mustelidae data could be bounded by the same sturdiness factor values that bound all the
740 other running/walking placental mammal data.

741

742

743
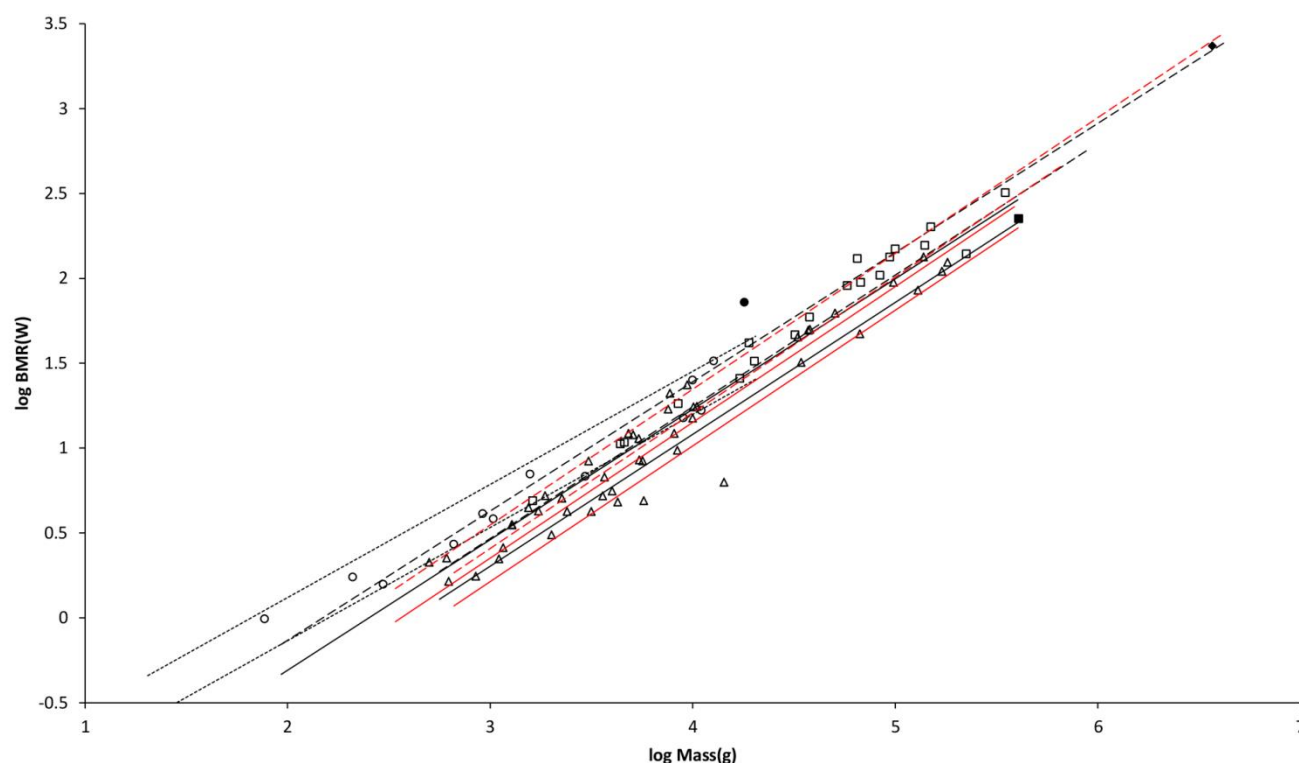
Figure 3. Log BMR as a function of log body mass for running/walking placental mammals. The *Elephas maximus* datum marked by a solid diamond is from (Savage et al, 2004). All other data are species-averages from (Kolokotrones et al, 2010).The solid, dashed and dotted lines are MMLE sturdiness factor boundaries. The upper boundaries were generated with a sturdiness factor $s = (3)^{0.5}$. The lower boundaries were generated with $s = (3)^{-0.5}$. The black lines are for $y = 2/3$. The colored lines are for $y = 0.8$. The steeper sloping boundary lines are for Froude-Strouhal dynamic similarity. The shallower sloping boundary lines are for geometric similarity. Ruminant Artiodactyla data are marked by open squares and R_M^2 is 0.9921 with respect to the dashed Froude-Strouhal black boundaries and R_M^2 is 0.9919 with respect to the dashed colored boundaries. *Camelius dromedarius* is a non-ruminant Artiodactyl marked by a solid square. Carnivora less Mustelidae data are marked with open triangles and R_M^2 is 0.9752 with respect to the solid Froude-Strouhal black boundaries and R_M^2 is 0.9655 with respect to the solid colored boundaries. Mustelidae except Enhydra data are marked with open circles and R_M^2 is 0.9999 with respect to the dotted geometric black boundaries. *Enhydra lutris* is an ocean going swimming Mustelid marked by a solid circle.

759

760 The Mustelidae data contained one sample for a sea otter (*Enhydra lutris*) which is an ocean
761 going swimmer rather than a runner/walker. Separating this sample from the rest of the
762 Mustelidae data leads to a slope of 0.69 as shown in table 1. This slope is not significantly
763 different from the geometric similarity slope of 0.67 as the log likelihood ratio for these slopes is
764 0.4. Geometric rather than Froude-Strouhal similarity supports separating Mustelidae fron the
765 rest of Carnivora for BMR analyses. Equations (3) with y = 2/3 and a geometric similarity
766 fundamental frequency of 1.4 (m/sec)/l and equation (2) are the MMLE equations for relating
767 BMR to body mass for geometric similarity. Of the constant parameters in these equations,
768 values applicable to Mustelidae for G_m, G_o, and G_r have been established. The MMLE
769 parameters that could be adjusted to account for the Mustelidae BMR deviation are the
770 fundamental propulsion frequency constant, c, the mitochondrion capability quotient, e and the
771 dynamic similarity constant, k. Because many Mustelidae combine swimming with terrestrial
772 locomotion it is possible that their skeletal musculature may not be dynamically similar to other
773 Carnivora and the constant k may be different from a value of 1.0. However, by equation (3), k
774 and c cannot be separated without additional information. The product kc and e were varied to
775 obtain the Mustelidae geometric similarity MMLE sturdiness factor boundaries shown in Fig. 3.
776 Using kc = 1.4 m/sec as was done for Proboscidae and Perissodactyla required a mitochondrion
777 capability quotient at least 170% of that applicable to other Carnivora. That a Mustelidae
778 mitochondrion would be this much more powerful than other carnivora mitochondria is difficult
779 to believe. Using a value of kc twice as large as that used for Perissodactyla and Proboscidae
780 reduced the required mitochondrion capability quotient to 130% of that for other Carnivora. An
781 implication would be that more powerful mitochondria allow Mustelidae to move their limbs
782 twice as fast as other placental mammals in performing routine locomotion tasks.

783 Coverage, R, is the fraction of samples that fall between the MMLE sturdiness boundaries.
784 Separating the Mustelidae from the rest of the Carnivora increased R for the entire Carnivora
785 order from about 0.44 to 0.53 for y = 2/3 and from about 0.39 to 0.49 for y = 0.8. Although
786 coverage is somewhat sparse, many of the samples lie close to the MMLE sturdiness boundaries
787 as the greater R_M^2 values indicate.

788 MMLE can exactly predict every individual body mass and shoulder height datum from (Nowak,
789 1999) for running/walking placental mammals that is shown in Fig. 1 and 2. There is no error
790 and thus no unexplained variance. Once the applicable skeletal muscle similarity is specified and
791 values for the constants G_m and G_o are established, computing an individual animal's mass from
792 its shoulder height only requires specifying its sturdiness factor. Mustelidae are an exception.
793 They require the further specification of a larger mitochondrion capability quotient, e, and an
794 appropriate combined fundamental propulsion frequency and dynamic similarity constants, kc.
795 As shown in Fig. 2 the differences are negligible between y = 2/3 which is indicated by the AVG
796 mass on characteristic length regression relationship and y = 0.8 which is indicated by the PI
797 mass on characteristic length regression relationship. The relationship between mass and

798 characteristic length for Proboscidae and Perissiodactyla may be better explained by geometric
799 similarity.

800 MMLE also can exactly predict every species-averaged BMR and mass datum from
801 (Kolokotrones et al, 2010) for running/walking placental mammals that are shown in Fig. 3 by
802 using equations (2) and (3) simultaneously. There is no error and thus no unexplained variance.
803 Body mass is computed with equation (3) as just described. Whether an animal is a ruminant
804 Artiodactyl or not needs to be specified to use the correct value of the constant G_r in equation (2)
805 to compute the animal's BMR from its shoulder height and sturdiness factor. Some iteration of
806 this process may be required if the characteristic length and/or sturdiness factor is not included
807 with the BMR and body mass data for the animal. As shown in Fig. 3 the differences in terms of
808 R_M^2 are negligible between y = 2/3 and y = 0.8.

809 **Rodentia.** Rodentia comprise about 20% of families, 39% of genera, and 43% of species of
810 recent mammals. Their masses range over four and a half orders of magnitude and their head and
811 body lengths range over one and a half orders of magnitude (*Mus minutoides* with a mass of 2.5g
812 and head and body length of 45mm to *Hydrochaeris hydrochaeris* with a mass of 79,000g and
813 head and body length of 1,300mm). Various species employ scurrying, climbing, gliding,
814 hopping, burrowing, swimming, running/walking , and combinations of these as their primary
815 means of locomotion (Nowak, 1999).

816 (Nowak, 1999) provides individual data on approximate minimum and maximum masses in
817 grams (g) and head and body lengths in millimeters (mm). The length data are mostly for genera
818 with very little data for species. There is also very little data on shoulder height. Given the
819 available data, linearly relating head and body length to characteristic length was tried. From the
820 reference (Nowak, 1999), 203 individual and 105 taxon-averaged mass, head and body length
821 samples were obtained (Data S2). (Kolokotrones et al, 2010) provides 267 species-averaged
822 BMR in watts (W) and mass in grams (g) samples. Table 2 shows the PI and AVG regression
823 analysis results obtained with this data. The length data was converted to meters (m) for
824 calculations involving equations (1) through (5).

825 Froude similarity should apply to skeletal muscle dynamics in most Rodentia as gravity is the
826 main force affecting their locomotion. This should be true even for swimming as aquatic
827 Rodentia are mainly surface swimmers that experience significant drag through the generation of
828 surface waves in the wake. Drag through the generation of surface waves in the wake is the
829 classic situation to which Froude similarity applies. What should govern the dynamics of
830 burrowing is not clear, but as will be seen Froude similarity seems to work. The mass regressed
831 on head and body length slope for both PI and AVG regressions for all families of Rodentia
832 trends toward the geometric slope of 3.0. The combination of all families except Cricetidae
833 trend toward an intermediate slope between the Froude-Strouhal slope of around 2.55 for
834 mammals the size of Rodentia and the geometric slope. Cricetidae have an AVG mass regressed
835 on length slope nearer the geometric similarity slope and the PI slope exceeds geometric

similarity. Cricetidae also have a PI BMR regressed on mass slope that is not significantly

different than the slope for geometric similarity as the log likelihood ratio for the slopes is 4.0.

_____

Table 2. Results of Regression Analyses for Rodentia.

Family	Regression Type	Independent Variable	Dependent Variable	Slope	Intercept	R^2	Number Samples
All Rodentia	PI(0.62)	Mass(g)	BMR(watts)	0.7231	-1.7198	0.8968	267
	PI(0.0)	Length(mm)	Mass(g)	2.9482	-4.3637	0.9571	105
	AVG	Length(mm)	Mass(g)	2.8692	-4.1497	0.9956	NA
Non-Cricetidae	PI(0.44)	Mass(g)	BMR(watts)	0.7399	-1.7685	0.9192	176
	PI(0.0)	Length(mm)	Mass(g)	2.9079	-4.2548	0.9571	78
	AVG	Length(mm)	Mass(g)	2.8564	-4.1124	0.9939	NA
Cricetidae	PI(0.55)	Mass(g)	BMR(watts)	0.6597	-1.5408	0.8497	91
	PI(0.0)	Length(mm)	Mass(g)	3.4061	-5.3367	0.9395	27
	AVG	Length(mm)	Mass(g)	2.9531	-4.3561	0.9908	NA

The regression expressions are: Log(dependent variable) = slope X log(independent variable) + intercept. PI(n) means the phylogenetic informed regression method using BayesTraits and the number in parentheses is the estimated value of lambda. AVG means the cohort averaging regression method. Length(mm) is head and body length in millimeters. Mass(g) is body mass in grams. NA means Not Applicable

_____

Besides appearing to be more geometrically similar, Cricetidae tend to have a higher BMR when compared to non-Cricetidae of the same mass. For these reasons Cricetidae were analyzed separate from all the other families of Rodentia.

The slope values for mass regressed on head and body mass in table 2 for both PI and AVG regressions are very different from the value of 2.5 obtained for y =0.8 for Artiodactyla + Carnivora. They indicate either geometric similarity with y = 2/3 or a mixture of geometric similarity and Froude-Strouhal similarity with y = 2/3. For non-Cricetidae, the PI regression slope is not significantly different from the AVG slope as the log likelihood ratio for the two slopes is less than 4.0. For these reasons y = 2/3 is used in equation (3) for Rodentia.

The characteristic length for Rodentia was assumed to be a constant fraction of head and body length. The fraction's value was estimated by equating the combined Artiodactyla and Carnivora mass regressed on length expression to the all families of Rodentia mass regressed on head and body length for the range of lengths for Rodentia. This results with a fraction that is within the range 0.4 to 0.62 using the PI regression relationship and 0.43 to 0.61 using the AVG relationship. A value of 0.5 was considered to be a reasonable working estimate for this characteristic length scaling fraction.

864 The characteristic length scaling fraction adds an additional parameter to the number that MMLE
865 uses to predict the absolute values of body mass and BMR. Its addition increases the total
866 number of parameters to 11.

867 The fundamental locomotion frequency for geometric similarity is a constant divided by the
868 characteristic length. The value of 1.4 m/sec for the constant that worked well for Perissodactyla
869 and Proboscidae was also used as the constant for Rodentia.

870 Figure 4 shows the MMLE mass as a function of head and body length sturdiness factor
871 boundaries for Froude-Strouhal dynamic similarity and geometric similarity evaluated with the
872 same constants that were used for running/walking mammals and a characteristic length scaling
873 factor of 0.5. The reference (Nowak, 1999) mass, head and body length samples for non-
874 Cricetidae Rodentia are also shown.

875 Figure 5 shows the MMLE BMR as a function of body mass sturdiness factor boundaries for the
876 two similarity regimes evaluated with the same constants that were used for non-Mustelidae
877 Carnivora and a characteristic length scaling factor of 0.5. The (Kolokotrones et al, 2010) BMR
878 and mass samples for non-Cricetidae Rodentia are also shown.

879 As with Mustelidae that have a greater BMR at the same body mass than do other Carnivora, a
880 greater mitochondrion capability quotient would most straight forwardly result in a greater BMR
881 for Cricetidae with the same masses as other Rodentia. This possibility was evaluated for
882 Cricetidae Rodentia. With all other parameters maintained identical to those used for
883 geometrically similar non-Cricetidae Rodentia, the mitochondrion capability quotient was varied
884 until a maximum value of R_M^2 was achieved for both mass as a function of length and BMR as a
885 function of mass. A mitochondrion capability quotient of 1.2 maximized the R_M^2 values. Figure
886 6 shows the MMLE mass as a function of head and body length sturdiness factor boundaries for
887 geometric similarity evaluated with this mitochondrion capability quotient value. The reference
888 (Nowak, 1999) mass, head and body length samples for Cricetidae Rodentia are also shown.
889 Figure 7 shows the MMLE BMR as a function of body mass sturdiness factor boundaries. The
890 reference (Kolokotrones et al, 2010) BMR and mass samples for Cricetidae Rodentia are also
891 shown.

892 Figure 6 shows that with the exception of a single outlier a tighter range of sturdiness factor for
893 the MMLE boundaries could embrace the Cricetidae mass, head and body length data. The
894 outlier is the larger sample of American harvest mice *(Reithrodontomys)*. However Fig. 7 shows
895 that the full sturdiness factor range is needed to embrace the Cricetidae BMR and mass data.

896 A mitochondrion capability quotient of 1.2 as an explanation of why Cricetidae have an elevated
897 BMR with respect to other Rodentia is considerably more palatable than the value of this
898 parameter needed to explain the elevated BMR of Mustelidae with respect to other Carnivora.

899
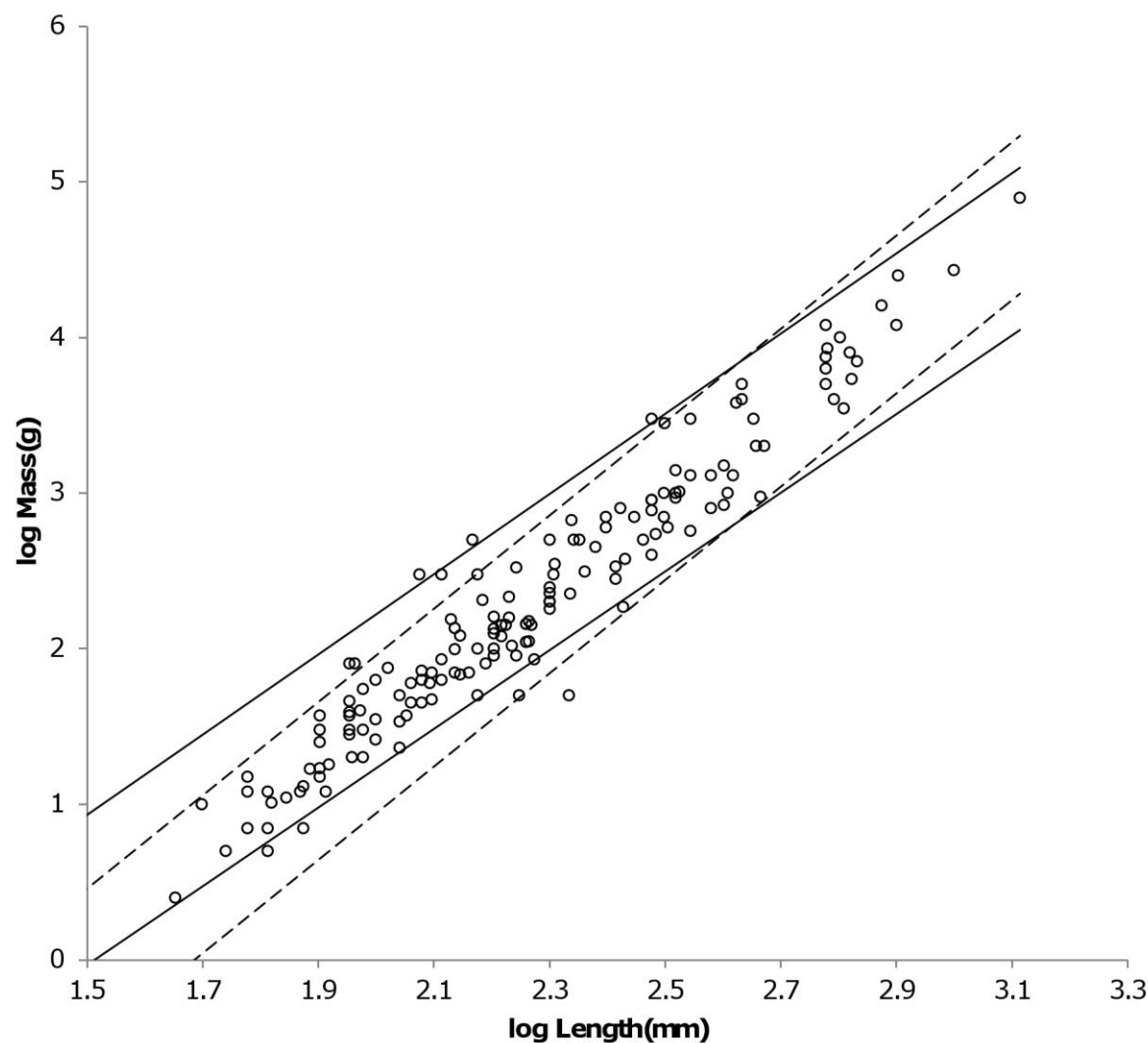
Figure 4. Log body mass as a function of log head and body length for non-Cricetidae Rodentia. Data are from (Nowak, 1999). The solid and dashed lines are MMLE sturdiness factor boundaries. The upper boundaries were generated with a sturdiness factor $s = (3)^{0.5}$. The lower boundaries were generated with $s = (3)^{-0.5}$. The shallower sloping solid boundary lines are for Froude-Strouhal similarity. The steeper sloping dashed boundary lines are for geometric similarity. The non-Cricetidae Rodentia individual mass, head and body length data are marked by open circles. $R_M^2 = 0.9995$ with respect to both sets of boundaries.

911

912
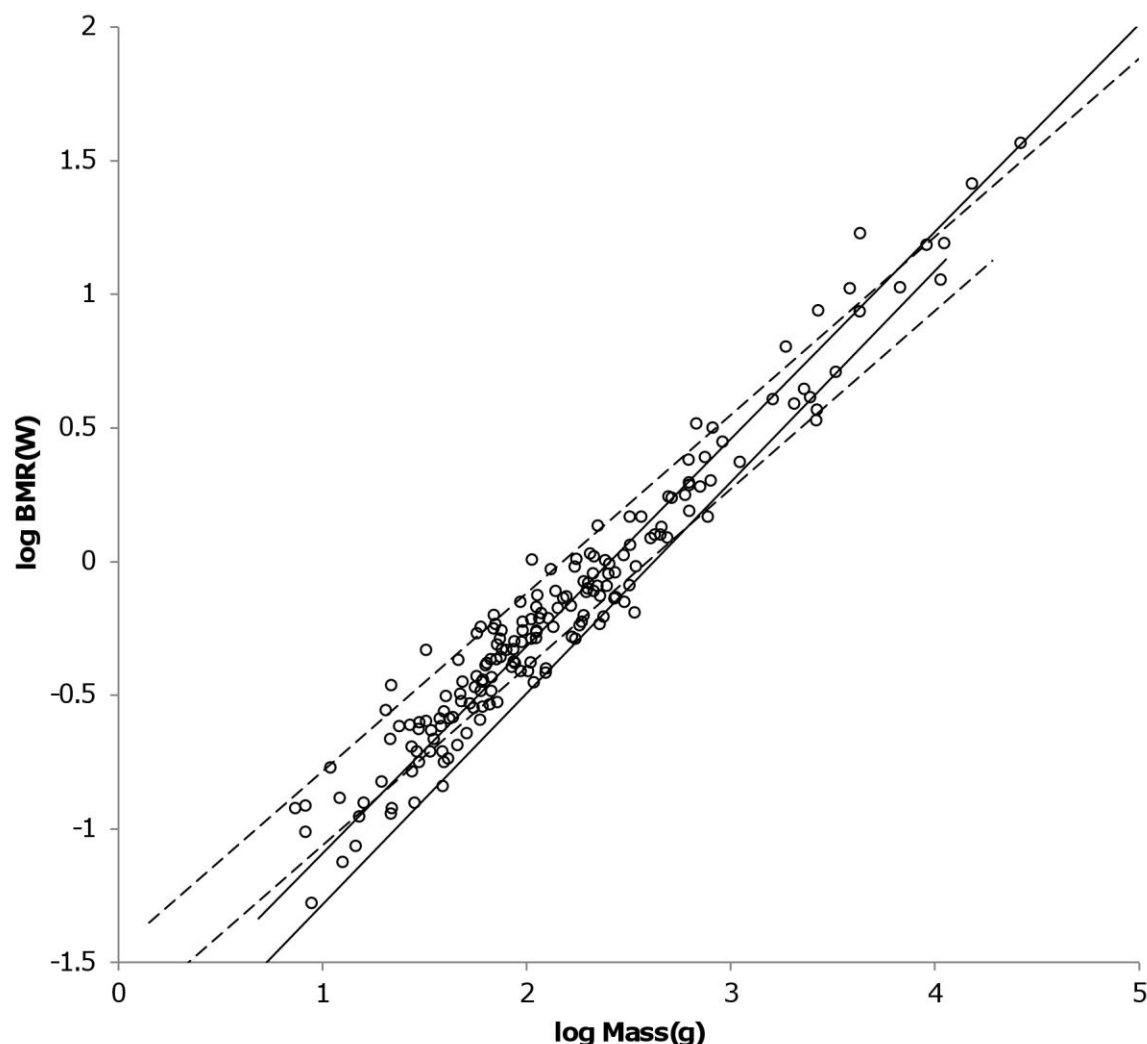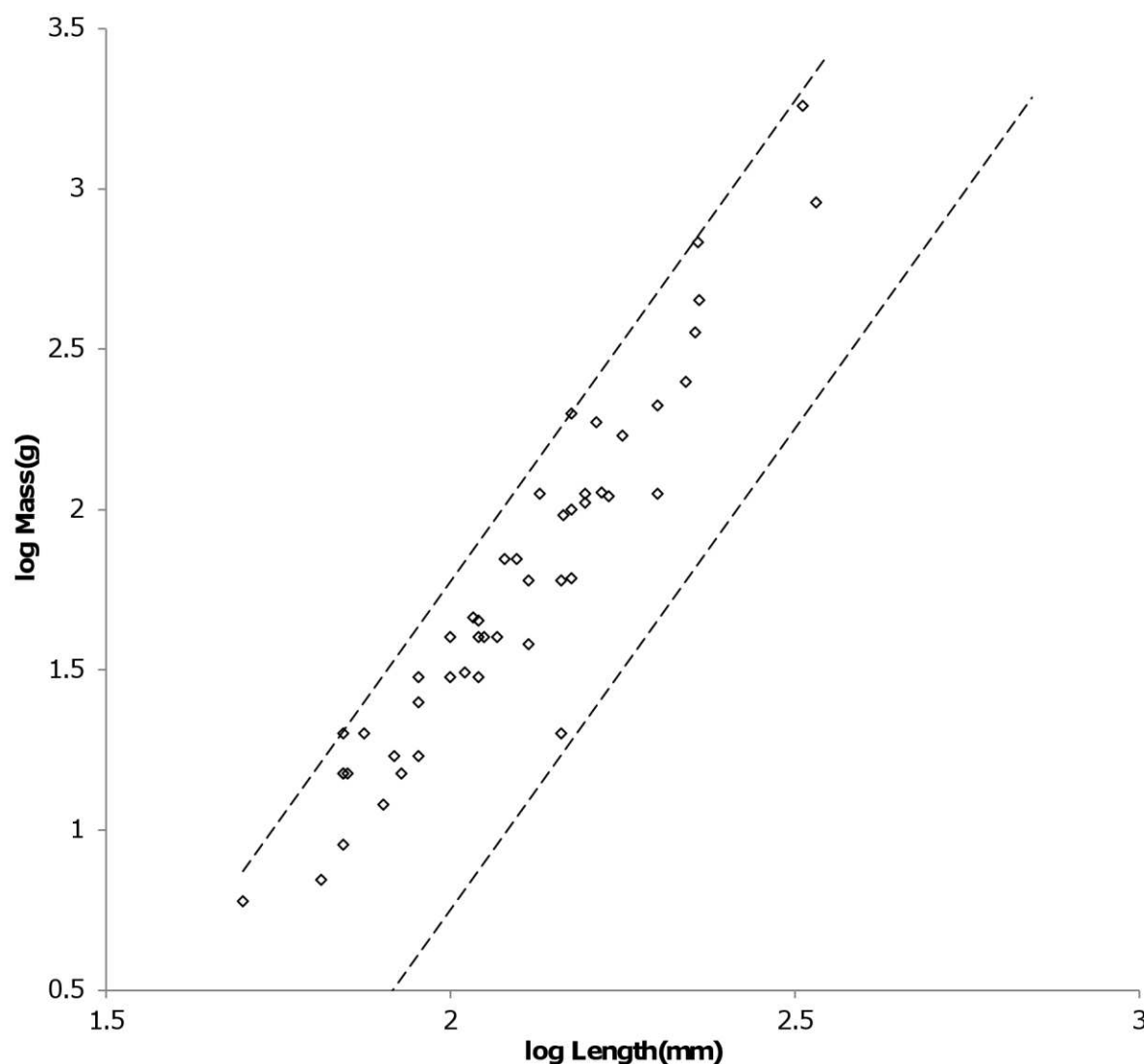
Figure 5. Log BMR as a function of log body mass for non-Cricetidae Rodentia. Data are
from (Kolokotrones et al, 2010). The solid and dashed lines are MMLE sturdiness factor
boundaries. The upper boundaries were generated with a sturdiness factor s = $(3)^{0.5}$. The lower
boundaries were generated with s = $(3)^{-0.5}$. The steeper sloping solid boundary lines are for
Froude-Strouhal similarity. The shallower sloping dashed boundary lines are for geometric
similarity. The species-averaged non-Cricetidae Rodentia mass, head and body length data are
marked by open circles. R_M^2 = 0.9966 with respect to both sets of boundaries.
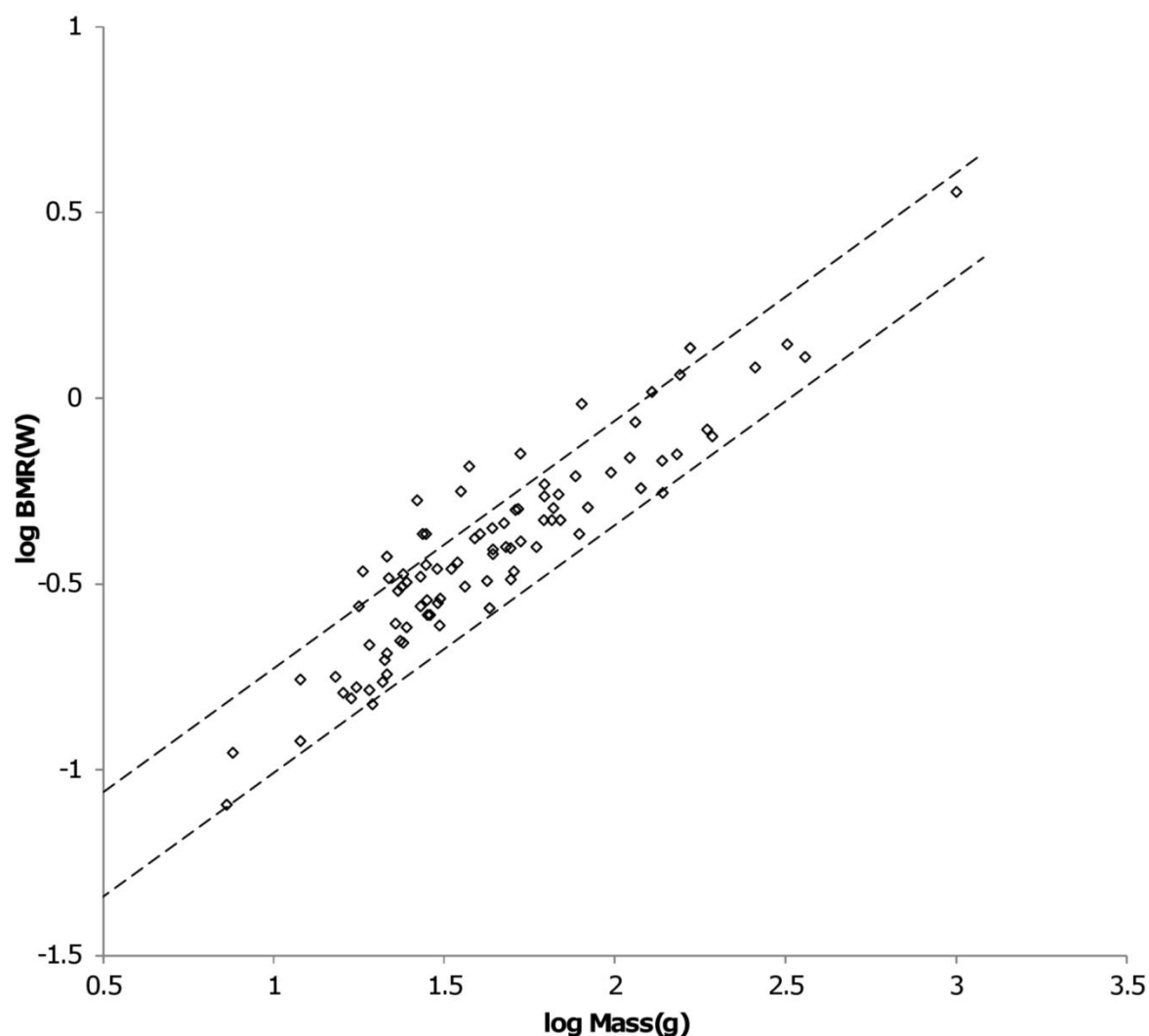
920

921

922

Figure 6. Log body mass as a function of log head and body length for Cricetidae Rodentia. The data are from (Nowak, 1999). The dashed lines are MMLE sturdiness factor boundaries. The upper boundary was generated with a sturdiness factor $s = (3)^{0.5}$. The lower boundary was generated with $s = (3)^{-0.5}$. The boundary lines are for geometric similarity. Cricetidae Rodentia individual mass, head and body length data are marked by open diamonds. $R_M^2 = 1.0$.

Figure 7. Log BMR as a function of log body mass for Cricetidae Rodentia. The Data are from (Kolokotrones et al, 2010). The dashed lines are MMLE sturdiness factor boundaries. The upper boundary was generated with a sturdiness factor $s = (3)^{0.5}$. The lower boundary was generated with $s = (3)^{-0.5}$. The boundary lines are for geometric similarity. The Cricetidae Rodentia species-averaged BMR, mass data are marked by open diamonds. $R_M^2 = 0.9913$.

MMLE can exactly predict every individual body mass, head and body length datum from (Nowak, 1999) for Rodentia that is shown in Fig. 4 and 6. There is no error and thus no unexplained variance. A characteristic length scaling fraction to translate the available head and body length data to characteristic length gives reasonable results. Then using the parameter values that were established for running/walking placental mammals, computing an individual non-Cricetid Rodent's mass from its characteristic length with equation (3) only requires specifying its sturdiness factor and its skeletal muscle similarity. Calculating a Cricetid Rodent's

body mass from its characteristic length with equation (3) requires specifying its sturdiness factor, geometric similarity and a larger mitochondrion capability quotient than that used for other Rodentia and non-Musteletid running/walking placental mammals.

MMLE can exactly predict every BMR and body mass datum from (Kolokotrones et al, 2010) for Rodentia that is shown in Fig. 5 and 7 by using equations (2) and (3) simultaneously. There is no error and thus no unexplained variance. Body mass is computed with equation (3) as just described. Then the non- ruminant Artiodactyl value of the constant G_r established for running/walking placental mammals is used in equation (2) to compute the Rodent's BMR from its shoulder height and sturdiness factor. Some iteration of this process may be required if the head and body length and/or sturdiness factor is not included with the BMR and body mass data for the animal.

Bats (the order Chiroptera). Bats are second only to rodents in the number of species among mammals. Bats comprise about 12% of families, 16% of genera, and 20% of species of recent Mammals. Their masses range over three orders of magnitude from *Craseonycteris thonglongyai* and *Tylonycteris pachypus* with masses as small as 2g to *Pteropus giganteus* with a mass of as much as 1600g. (Nowak, 1999).

(Nowak, 1999) provides data in grams (g) for approximate minimum and maximum body masses. It also provides in millimeters (mm) approximate head and body lengths, forearm lengths and tail lengths when a tail is present. The data are mostly for genera with very little data for species. There is little data on wing span. From the reference (Nowak, 1999) data 350 individual and 176 taxon-averaged body mass, head and body length and forearm length samples were obtained (Data S3). (Kolokotrones et al, 2010) provides 85 species-averaged BMR and body mass samples. BMR is given in watts and mass is given in grams (g). Lengths were converted to meters (m) for calculations involving equations (1) through (5).

Bats primary means of locomotion is flying by flapping very flexible membranous wings controlled by multi-jointed fingers (Muijres et al, 2011). Unlike birds, bats use their hind limbs as well as their fore limbs to flap their wings (Norberg, 1981). Bats experience daily and seasonal fluctuations in body mass which they accommodate by changes in wing kinematics that vary among individuals (Iriarte-Diaz et al, 2012). To analyze the applicability of MMLE theory to bats, a characteristic length and a fundamental propulsion frequency related to very complicated flapping wing flight needed to be identified. The characteristic length should be related to wing dimensions. (Norberg, 1981) found that forearm length scaled with body mass with about the same exponent as wing span. Given the options available with the (Nowak, 1999) data, it was assumed that forearm length is linearly related to characteristic length. A possible complication that is avoided by this assumption is that full wing dimensions, such as wing span, in a flying bat may vary with flight mode and speed and may be different than those measured from specimens stretched out flat on a horizontal surface (Riskin et al, 2010).

984 (Norberg & Rayner, 1987) found that geometric similarity applied for most bat wing dimensions
985 with some exceptions. More recent work suggests that wing bone lengths are also geometrically
986 similar with respect to body mass in different sized bats (Norberg & Norberg, 2012).

987 The order Chiroptera is divided into two suborders: the Megachiroptera consisting of the single
988 family Peteropodidae and the Microchiroptera consisting of all other bats (Nowak, 1999). Table
989 3 shows the PI and AVG regression analysis results obtained with the (Nowak, 1999) forearm
990 length data and the (Kolokotrones et al, 2010) BMR data for all bats and for the two suborders
991 considered separately. y = 2/3 is consistent with both the PI and AVG all bats results and the
992 Megachiroptera results. y = 0.8 is consistent with both PI and AVG results for Microchiroptera.

993
994
995 _____
996
997 **Table 3.** Results of Bat regression Analyses

Order or Family	Regression Type	Independent Variable	Dependent Variable	Slope	Intercept	R^2	Number Samples
All Bats	PI(0.93)	Length(mm)	Mass(g)	2.6668	-3.3211	0.8507	176
	AVG	Length(mm)	Mass(g)	2.7718	-3.3628	0.9924	NA
Megachiroptera	PI(0.33)	Length(mm)	Mass(g)	2.8628	-3.4933	0.9749	40
	AVG	Length(mm)	Mass(g)	2.7335	-3.2632	0.9978	NA
Microchiroptera	PI(0.93)	Length(mm)	Mass(g)	2.515	-3.1025	0.7522	136
	AVG	Length(mm)	Mass(g)	2.5292	-2.9844	0.9928	NA
Heavy Bats	PI(0.79)	Length(mm)	Mass(g)	2.7595	-3.3252	0.922	86
	AVG	Length(mm)	Mass(g)	2.7233	-3.2329	0.9937	NA
Light Bats	PI(0.0)	Length(mm)	Mass(g)	3.28	-4.4926	0.8781	29
	AVG	Length(mm)	Mass(g)	2.9878	-3.9552	0.9743	NA
All Bats	PI(0.83)	Mass(g)	BMR(watts)	0.8111	-1.9063	0.8784	84
Megachiroptera	PI(0.56)	Mass(g)	BMR(watts)	0.8581	-2.0161	0.9279	21
Microchiroptera	PI(1.07)	Mass(g)	BMR(watts)	0.7459	-1.8247	0.991	63
Heavy Bats	PI(0.89)	Mass(g)	BMR(watts)	0.8225	-1.9166	0.8887	51
Light Bats*	PI(0.0)	Mass(g)	BMR(watts)	0.7015	-1.8048	0.8154	17

998

999 The regression expressions are: Log(dependent variable) = slope X log(independent variable) +
1000 intercept. PI(n) means the phylogenetic informed regression method using BayesTraits and the
1001 number in parentheses is the estimated value of lambda. AVG means the cohort averaging
1002 regression method. Length(mm) is forearm length in millimeters. Mass(g) is body mass in
1003 grams. NA means Not Applicable. *Data available for only 4 of the 8 families comprising light
1004 bats.

1005 _____

1006 Figure 8 offers an alternative partitioning for bats in which the bat families have been divided
1007 into three groups: 'heavy' bats, 'light' bats and 'intermediate' bats. At the same forearm length
1008 members of families composing the heavy bats are mostly more massive than those of the

1009 families composing the light bats. Intermediate bats span both the heavy and light mass regimes.
1010 The families composing the three groups are given in the caption of Fig. 8.

1011 _____

1012
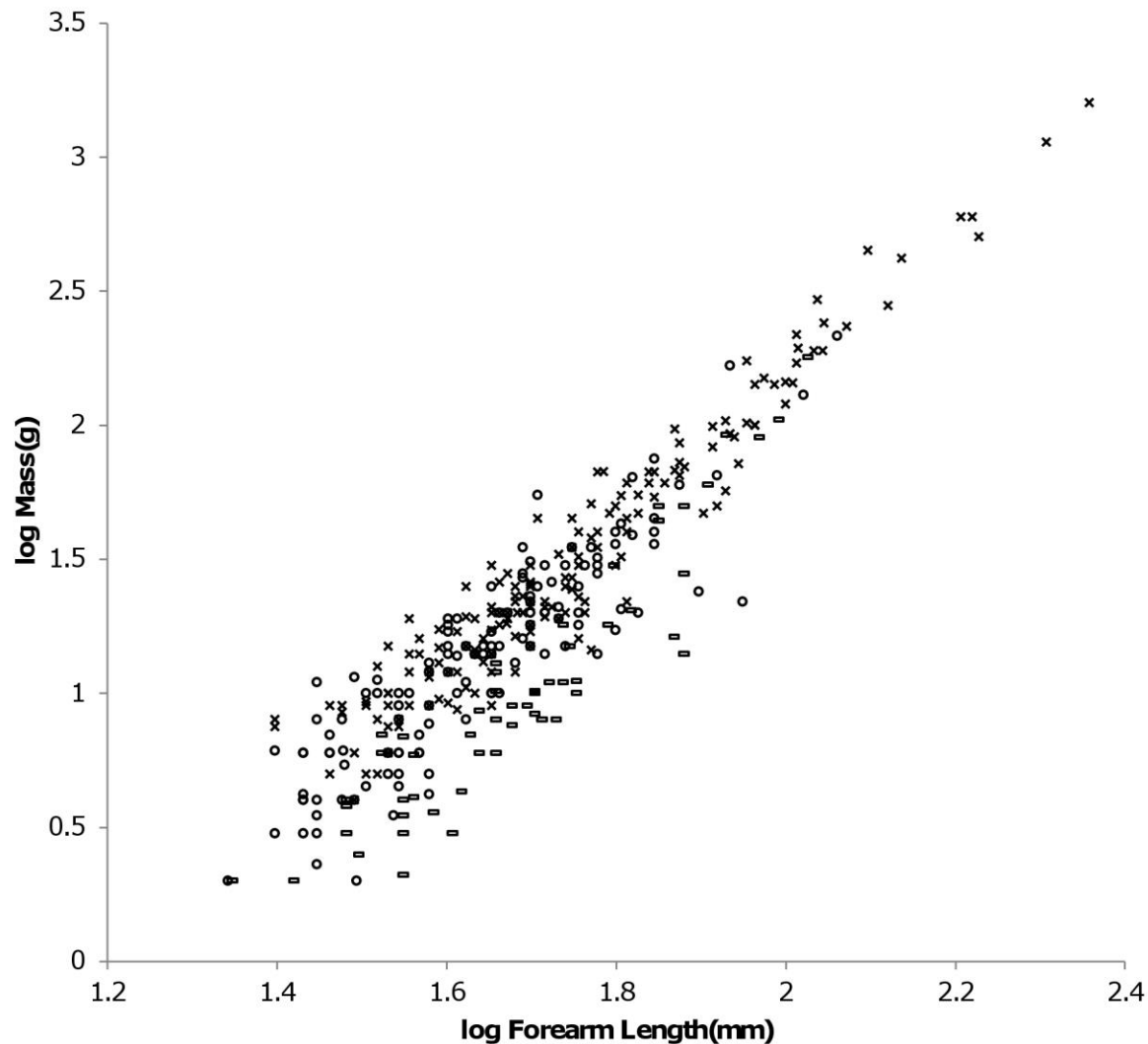
1013 **Figure 8. Log body mass as a function of log forearm length for bats.** Data are from (Nowak,
1014 1999). At the same forearm length individuals from families composing the 'heavy' bats marked
1015 with Xes are mostly more massive than those from the families composing the 'light' bats
1016 marked with open rectangles. 'Intermediate' bats marked with open circles span both the heavy
1017 and light mass regimes. The families Pteropodidae and Phyllostomidae comprise the heavy bats.
1018 The families Emballonuridae, Craseonycteridae, Rhinopomatidae, Rhinolophoidea,
1019 Mormoopidae, Noctilionidae, Furipteridae and Hipposideridae comprise the light bats. The
1020 families Nycteridae, Megadermatidae, Vespertilionoidea, Thyropteridae, Myzopodidae,
1021 Natalidae, Mystacinidae, and Molossidae comprise the intermediate bats.

1022 _____

1023 For the AVG regression of log mass on log forearm length the slope for light bats is very nearly
1024 the 3.0 expected for geometric similarity and the slope of the PI regression relationship is not
1025 significantly different from 3.0 as the log likelihood ratio is only 2.7. Light bats appear to be
1026 geometrically similar.

1027 Pteropodidae and Phyllostomidae comprise the heavy bats. The Pteropodidae contain the Old
1028 World frugivores and the Phyllostomidae contain the New World frugivores. While both families
1029 have species with other diets, the frugivores have wings adapted to commuting long distances
1030 from roost to feeding areas (Norberg & Rayner, 1987).The relationships between wing
1031 dimensions and body mass should be similar for the frugivore members of the two families.

1032 The fundamental propulsion frequency for bats should be related to the wing flapping frequency.
1033 A bat's wing flapping frequency increases slightly with air speed at lower speeds. It becomes
1034 almost independent of speed at higher speeds. The speed at which the transition occurs is the
1035 preferred speed (Bullen & McKenzie, 2002). The wing flapping frequency at this preferred speed
1036 should be proportional to the fundamental propulsion frequency.

1037 Animals that fly by flapping wings operate in a narrow range of Strouhal numbers in cruising
1038 flight (Taylor, Nudds & Thomas, 2003). Strouhal number does not change significantly for
1039 Pteropodidae (Riskin et al, 2010). It appears to be an accurate predictor of wingbeat frequency
1040 for birds (Nudds, Taylor & Thomas, 2004). Strouhal dynamic similarity should apply to bats.

1041 As noted in the summary of MMLE theory the fundamental frequency of propulsion would be
1042 proportional to the inverse square of the characteristic length if both Strouhal and Reynolds
1043 dynamic similarity applied simultaneously. By equation (3) this would result in body mass being
1044 proportional to the characteristic length raised to a power greater than 3. This situation is not
1045 observed in the Table 3 regression results except for PI mass regressed on forearm length for
1046 light bats. However since the AVG result is so close to geometric similarity and the difference
1047 between the PI result and geometric similarity is not significant, this was interpreted as support
1048 for geometric similarity with y = 2/3 as was done with Cricetidae Rodentia. It is noted that the
1049 characteristic length for viscous drag and that for vortex growth and shedding could be different
1050 body dimensions.

1051 For bats Strouhal number = (wingbeat frequency)X(wingbeat amplitude)/(air speed). Wingbeat
1052 amplitude is the vertical distance the wing tip travels during a stroke. Under Strouhal dynamic
1053 similarity the wingbeat amplitude should be proportional to the MMLE characteristic length. It
1054 was assumed that wingbeat amplitude characteristic length is a fraction of forearm length for
1055 bats. Further analysis involving maximization of R_M^2 for light bat BMR resulted with
1056 characteristic length = 0.61 of forearm length, kc = 0.625 m/sec and R_M^2 = 0.9984 (see Article
1057 S1).

1058 Strouhal dynamic similarity is consistent with geometric similarity. Since the fundamental
1059 propulsion frequency under geometric similarity is proportional to the inverse of the

1060 characteristic length, simultaneous geometric and Strouhal similarity imply that the preferred
1061 flight speed is approximately constant.

1062 Since R^2 is nearly unity for the AVG regression relationship of Table 3, equation (6) should
1063 apply. The log likelihood for the resulting exponent, $2/x = 0.6694$ could not be calculated using
1064 BayesTraits. Thus the significance of its difference from the BMR regressed on mass exponent
1065 in Table 3 could not be determined. It is noted that length and mass data was available from
1066 (Nowak, 1999) to estimate x from for all families composing the light bats group but BMR and
1067 mass data from (Kolokotrones et al, 2010) to estimate the BMR regressed on mass exponent was
1068 available for only four of the eight families.

1069 Figure 9 shows the MMLE BMR as a function of body mass boundaries for geometric similarity
1070 for light bats evaluated with these estimates together with the (Kolokotrones et al, 2010) BMR
1071 and body mass samples for light bats.

1072 A methodology similar to that used for light bats was used to establish the characteristic length
1073 scaling fraction and fundamental propulsion frequency constant for heavy bats. By the heavy bat
1074 regression relationships of table 3, heavy bats are not geometrically similar. Since heavy bats are
1075 not geometrically similar the exponent, r, in the relationship between fundamental propulsion
1076 frequency and characteristic length in equations (3) and (5) also had to be established. The
1077 results using the Table 3 AVG relationships were characteristic length = 0.92 forearm length, r =
1078 0.68, kc = 3.22 $m^{0.68}$/sec and R_M^2 for BMR = 0.9828. The results using the PI relationships were
1079 characteristic length = 0.86 forearm length, r = 0.73, kc = 2.59 $m^{0.73}$/sec, and R_M^2 for BMR =
1080 0.9918. In terms of R_M^2 the PI and AVG results are nearly indistinguishable (see Article S1).

1081 Since R^2 is nearly unity for the heavy bat AVG mass regressed on length relationship in Table 3,
1082 equation (6) should apply. The difference between the resulting exponent, $2/x = 0.7344$ and the
1083 PI BMR regressed on mass exponent in Table 3 is borderline significant as the log likelihood
1084 ratio is 4.1.

1085 Figure 9 also shows the MMLE log BMR as a function of log body mass MMLE sturdiness
1086 factor boundaries for heavy bats evaluated with these estimates together with the (Kolokotrones
1087 et al, 2010) species-averaged BMR and body mass samples for heavy bats.

1088 Figure 10 shows the MMLE log body mass as a function of log forearm length MMLE sturdiness
1089 factor boundaries for both heavy bats and geometrically similar light bats. The (Nowak, 1999)
1090 heavy and light bat mass and forearm length data are also shown.

1091

1092

1093
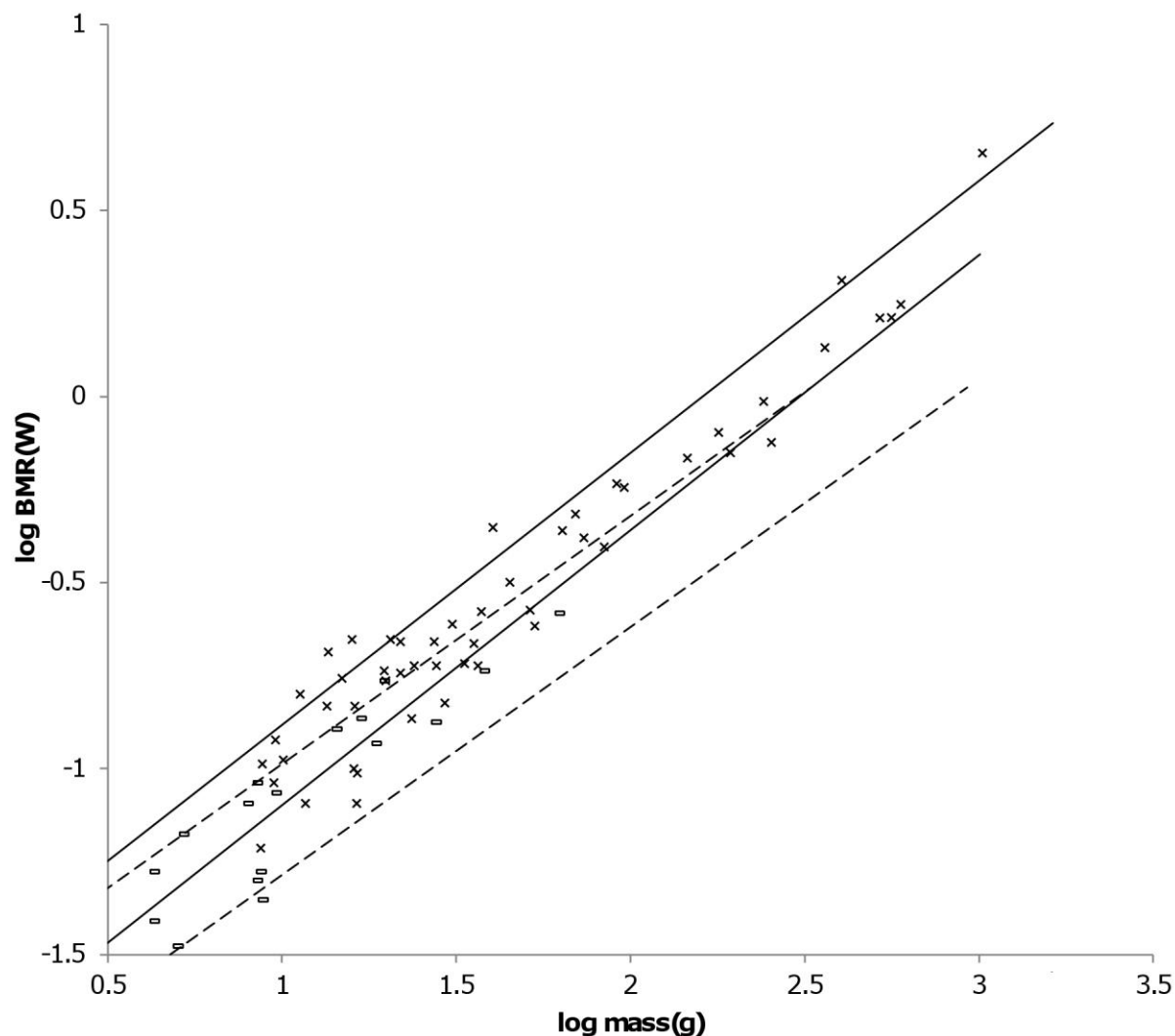
Figure 9. Log BMR as a function of log body mass for heavy and light bats. Data are from
(Kolokotrones et al, 2010). The solid and dashed lines are the MMLE sturdiness factor
boundaries. The upper boundaries were generated with a sturdiness factor $s = (3)^{0.5}$. The lower
boundaries were generated with $s = (3)^{-0.5}$. The steeper sloping solid boundary lines are for heavy
bat Strouhal dynamic similarity. The shallower sloping dashed boundary lines are for light bat
geometric similarity. $R_M^2 = 0.9828$ for heavy bats with respect to the Strouhal boundaries. $R_M^2 =$
0.9984 for light bats with respect to the geometric boundaries. Heavy bat species-averaged data
are marked with Xes. Light bats species-averaged data are marked with open rectangles. Data
was available for only four of the eight families comprising the light bats.

1094
1095
1096
1097
1098
1099
1100
1101
1102

1103

1104
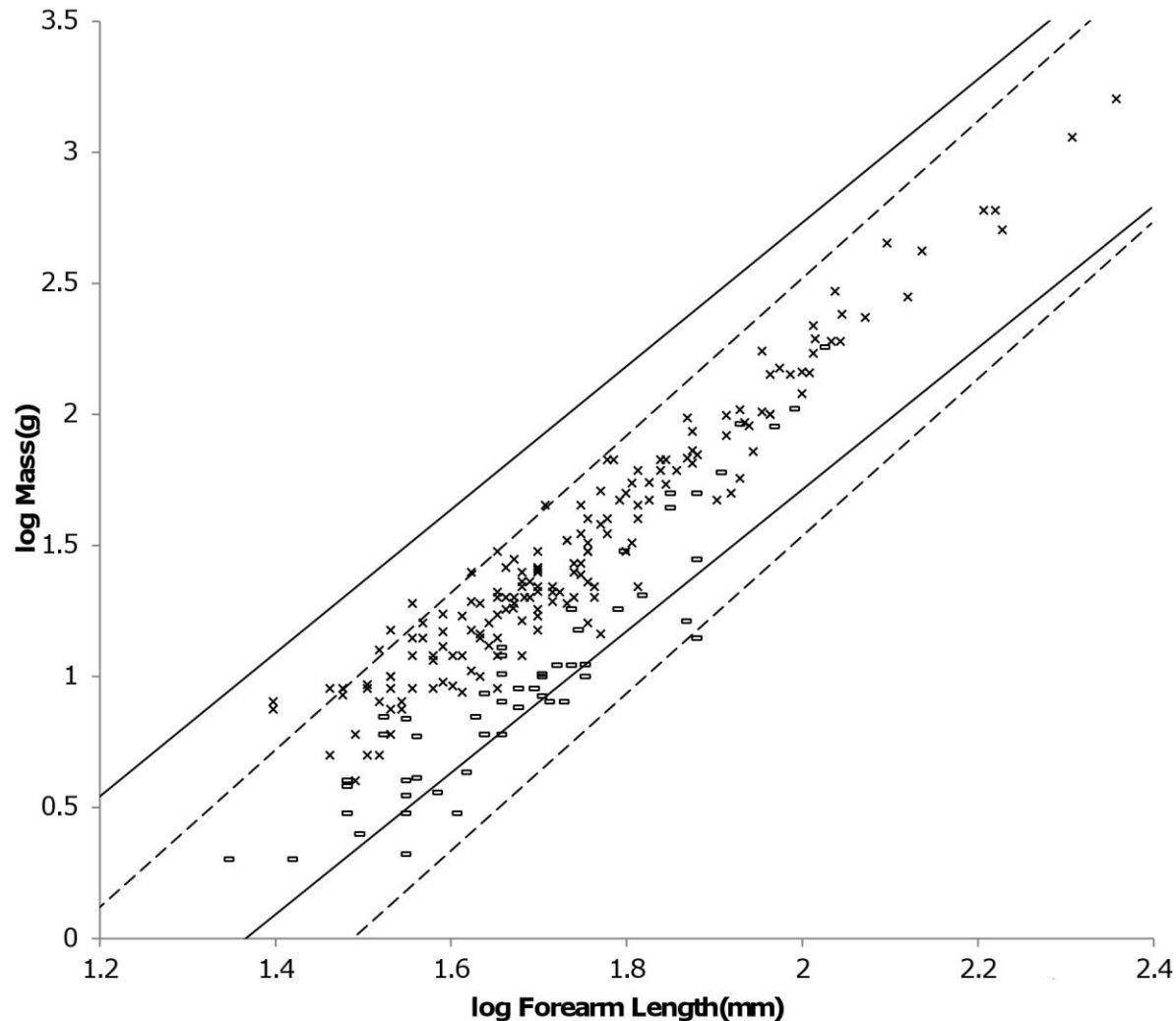
Figure 10. Log body mass as a function of log forearm length for heavy and light bats. Data are from (Nowak, 1999). The solid and dashed lines are the MMLE sturdiness factor boundaries. The upper boundaries were generated with a sturdiness factor $s = (3)^{0.5}$. The lower boundaries were generated with $s = (3)^{-0.5}$. The shallower sloping solid boundary lines are for heavy bat Strouhal dynamic similarity. The steeper sloping dashed boundary lines are for light bat geometric similarity. $R_M^2 = 0.9982$ for heavy bats with respect to the Strouhal boundaries. $R_M^2 = 1.0$ for light bats with respect to the geometric boundaries. Individual heavy bats are marked with Xes. Individual light bats are marked with open rectangles.

Figure 11 shows the MMLE log BMR as a function of log body mass MMLE sturdiness factor boundaries for both heavy bats and light bats. The (Kolokotrones et al, 2010) species averaged BMR and body mass samples for intermediate bats are also shown. The data spreads over both

1119 MMLE bands as if within the same family there are species that conform to geometric similarity
1120 and other species that conform to heavy bat similarity.

1121 Figure 12 shows the MMLE log body mass as a function of log forearm length MMLE sturdiness
1122 factor boundaries for both heavy and light bats. The (Nowak, 1999) body mass and forearm
1123 length samples for intermediate bats are also shown. Intermediate bat body mass is explained
1124 almost equally well by either the geometrically similar light bat MMLE band or the heavy bat
1125 MMLE band. $R_M^2 = 0.9981$ for the light bat MMLE band. $R_M^2 = 0.9980$ for the heavy bat
1126 MMLE band. $R_M^2 = 0.9999$ for the two bands together.

1127 The light and heavy bat data in Fig. 10 does not fully occupy their respective MMLE sturdiness
1128 factor bands. This raises the possibility that a sturdiness factor range narrower than $(3)^{-0.5}$ to $(3)^{0.5}$
1129 may apply to heavy or light bats. The intermediate bat data in Fig. 12 more completely occupies
1130 both bands indicating that the full sturdiness factor range is applicable. The situation may be
1131 more complicated. Each of the heavy, light and intermediate bat groups contains species with
1132 different food habits. Bat wing morphology is associated with flight behavior related to food
1133 habits. Even among the insectivores that dominate the light and intermediate groups there are
1134 different styles of catching insects that are associated with differing wing morphologies (Norberg
1135 & Rayner, 1987; Norberg & Norberg, 2012). Dynamic similarity may apply at a phylogenetic
1136 level below the family.

1137 The light-intermediate-heavy representation of bats is better supported by the data than either the
1138 all bats representation or the Megachiroptera-Microchiroptera representation in terms of R_M^2 and
1139 coverage, R (see Article S1).

1140 MMLE can exactly predict every body mass, head and body length datum from (Nowak, 1999)
1141 for bats that is shown in Fig. 8, 10 and 12. There is no error and thus no unexplained variance. A
1142 separate characteristic length scaling fraction is needed for light bats and for heavy bats to
1143 translate the available forearm length data to characteristic lengths. Then using the parameter
1144 values that were established for running/walking placental mammals, computing an individual
1145 light bat's body mass from its forearm length with equation (3) requires specifying its sturdiness
1146 factor, geometric muscle similarity and the light bat combined fundamental propulsion frequency
1147 and dynamic similarity constants, kc. Computing a heavy bat's body mass from its forearm
1148 length with equation (3) requires specifying its sturdiness factor, the heavy bat fundamental
1149 propulsion frequency exponent, r, and the heavy bat combined fundamental propulsion
1150 frequency and dynamic similarity constants, kc. Computing an intermediate bat's body mass
1151 from its forearm length may require evaluating the animal as a light bat and as a heavy bat and
1152 then deciding which classification better agrees with the datum

1153

1154
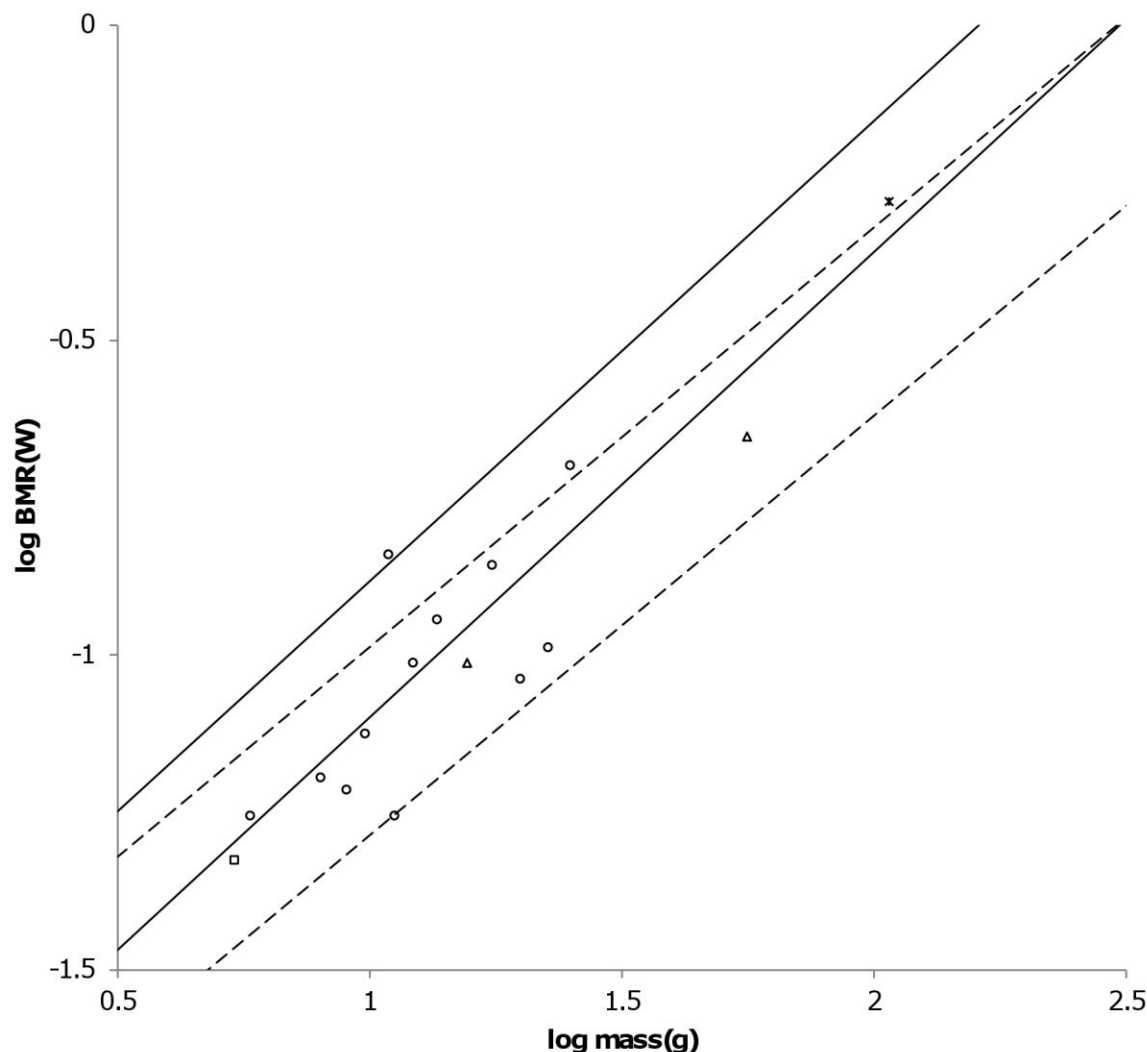
Figure 11. Log BMR as a function of log body mass for intermediate bats. Data are from
(Kolokotrones et al, 2010). The solid and dashed lines are the MMLE sturdiness factor
boundaries. The upper boundaries were generated with a sturdiness factor $s = (3)^{0.5}$. The lower
boundaries were generated with $s = (3)^{-0.5}$. The steeper sloping solid boundary lines are for heavy
bat Strouhal dynamic similarity. The shallower sloping dashed boundary lines are for light bat
geometric similarity. Data was available for only four of the eight families comprising the
intermediate bats. $R_M^2 = 0.9678$ for intermediate bats with respect to the Strouhal boundaries.
$R_M^2 = 0.9893$ for intermediate bats with respect to the geometric boundaries. $R_M^2 = 0.9998$ for
intermediate bats with respect to both sets of boundaries. The data are species-averaged.
Megadermatidae are marked with crossed Xes. Molossidae are marked with open triangles.
Vesperstilionidae are marked with open circles. Natalidae are marked with open squares.

1169

1170
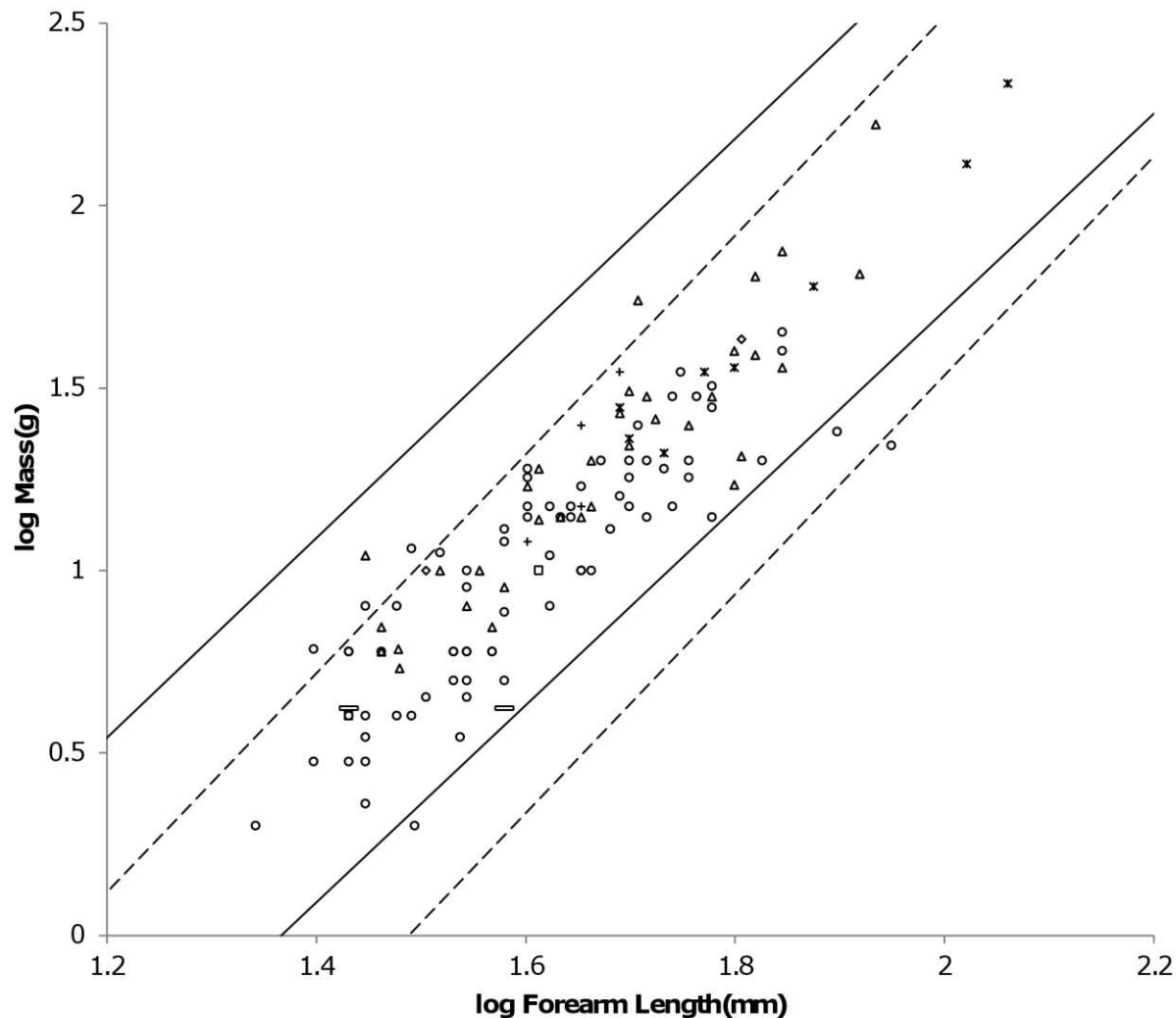
Figure 12. Log body mass as a function of log forearm length for intermediate bats. Data
are from (Nowak, 1999). The solid and dashed lines are the MMLE sturdiness factor boundaries.
The upper boundaries were generated with a sturdiness factor $s = (3)^{0.5}$. The lower boundaries
were generated with $s = (3)^{-0.5}$. The shallower sloping solid boundary lines are for heavy bat
Strouhal dynamic similarity. The steeper sloping dashed boundary lines are for geometric
similarity. $R_M^2 = 0.998$ for intermediate bats with respect to the Strouhal boundaries. $R_M^2 =$
0.9981 for intermediate bats with respect to the geometric boundaries. $R_M^2 = 0.9999$ for
intermediate bats with respect to both sets of boundaries.

1171
1172
1173
1174
1175
1176
1177
1178

1179

1180

1181

1182 MMLE can also predict every BMR and body mass datum from (Kolokotrones et al, 2010) for
1183 bats that is shown in Fig. 9 and 11 by using equations (2) and (3) simultaneously. There is no
1184 error and thus no unexplained variance. Body mass is computed with equation (3) as just
1185 described. Then the Carnivore value of the constant G_r established for running/walking placental
1186 mammals is used in equation (2) to compute the bat's BMR from its forearm length and
1187 sturdiness factor. Some iteration of this process may be required if the head and body length
1188 and/or sturdiness factor is not included with the BMR and body mass data for the animal.

1189 **Discussion.** For an individual animal that has a particular characteristic length and a particular
1190 sturdiness factor, MMLE can deterministically predict with equation (3) the absolute value of its
1191 body mass rather than a statistical best fit average value for a collection of individuals from its
1192 species for at least the placental mammal orders Rodentia, Chiroptera, Artiodactyla, Carnivora,
1193 Perissodactyla and Proboscidae. There is no error and thus no unexplained variance. Furthermore
1194 MMLE can deterministically predict with equation (2) the absolute value of BMR for the
1195 individual animal rather than a statistical best fit average value for a collection of individuals
1196 from its species for at least the placental mammal orders Rodentia, Chiroptera, Artiodactyla,
1197 Carnivora. There is no error and thus no unexplained variance.

1198 Looked at another way, sturdiness factors can be found so that MMLE can deterministically
1199 predict with equation (3) every mass and length datum in the (Nowak, 1999) data set for the
1200 placental mammal orders that are addressed in this paper without error or unexplained variance.
1201 Characteristic lengths and sturdiness factors can be found so that MMLE can deterministically
1202 predict every BMR and mass datum in the (Kolokotrones et al, 2010) data set without error or
1203 unexplained variance.

1204 The ability of MMLE to exactly predict every datum obtained from the appropriate data set does
1205 not necessarily mean that there is no unexplained variance with MMLE theory. Equations (2)
1206 and (3) apply simultaneously to a particular individual animal which has particular values for
1207 body mass, BMR, and characteristic length. The author of the present paper is unaware of a data
1208 set that reports all three of these values for individual animals. Instead there is the data set from
1209 (Nowak, 1999) reporting individual body mass and characteristic length and another data set
1210 from (Kolokotrones et al, 2010) that reports species-averaged BMR and body mass. It is unlikely
1211 that the same particular animal is included in both data sets. There is likely to be unexplained
1212 variance with a data set that simultaneously reports the three values of mass, BMR and length for
1213 individual animals. The unexplained variance would be detected by the need to use one value of
1214 the sturdiness factor in equation (3) to accurately predict mass and a different value in
1215 equation(2) to accurately predict BMR for the same animal.

1216 However, as shown in Table 4, MMLE is able to predict the BMR regressed on mass exponent
1217 obtained by PI regression analysis of the (Kolokotrones et al, 2010) BMR and mass data from
1218 the mass regressed on length exponent obtained by AVG regression analysis of the (Nowak,
1219 1999) length and mass data for many of the MMLE phylogenetic homogeneous groups

1220 addressed in this paper. This is a result of being able to use equation (6) because R^2 is nearly
1221 unity for the AVG regression analyses. This might not be significant for the multiplicative
1222 constants in equations (2) and (6) as the regression analyses for both data sets were used to
1223 estimate the value of G_r that occurs in both equations. But the exponents are independent of the
1224 multiplicative constants. These considerations argue that MMLE may be able to simultaneously
1225 predict an individual animal's mass and BMR given its characteristic length and sturdiness
1226 factor; or looked at another way, it may be possible to find sturdiness factors so that MMLE can
1227 predict every datum form a data set that simultaneously reports individual animals mass,
1228 characteristic length and BMR.

1229 _____

1230 **Table 4.** Comparison of the theoretical value of the exponent, b, with the value obtained by PI
1231 regression analysis for the equation $BMR = aW^b$ for MMLE phylogenetic homogeneous groups.

MMLE Phylogenetic Homogeneous Group	Exponent From PI Regression Analysis, b	Theoretical exponent	Log Likelihood Ratio	Significant Difference?
Carnivora less Mustelidae	0.758	0.7651[2]	0.1	N
Ruminant Artiodactyla	0.7805	0.7651[2]	2.8	N
Mustelidae less Enhydra	0.6852	0.6667[1]	0.4	N
Cricetidae Rodentia	0.6597	0.6773[2]	17.8	Y
Cricetidae Rodentia	0.6597	0.6667[1]	4.0	N
Heavy Bats	0.8225	0.7344[2]	4.1	Y/N
Light Bats	0.7015	0.6694[2]	NC	NC

1232

1233 The exponents from PI regression analyses, b, are the slope values reported in Tables 1 through 3
1234 for the PI regression type with independent variable Mass(g) and dependent variable
1235 BMR(watts). The theoretical exponent is either (1) the value assuming geometric similarity or
1236 (2) the equation (6) value, 2/x, where x is the slope value reported in tables 1 through 3 for the
1237 AVG regression type with independent variable Height(m) or Length(mm) and dependent
1238 variable Mass(g). The values for x were obtained by analyses of data from (Nowak, 1999) by the
1239 cohort averaging regression method (AVG). The PI regression analysis exponents were obtained
1240 by Phylogenetically Informed (PI) regression analyses of (Kolokotrones et al, 2010) data using
1241 BayesTraits. A log likelihood ratio less than 4.0 means that an exponent from the PI regression
1242 analysis column is not significantly different from the corresponding exponent from the
1243 theoretical exponent column (Pagel, 1999). N means "no", Y means "yes" and Y/N means
1244 borderline. NC means that a log likelihood ratio could not be calculated for the Light Bats group.

1245 _____

1246 Non-Crecetidae Rodentia are not included in Table 4 because they are composed of mixtures of
1247 Froude-Strouhal and geometric similar animals and thus are not MMLE phylogenetic

1248   homogeneous groups. Intermediate bats are not included because they are composed of a mixture
1249   of animals with heavy bat and/or light bat MMLE features.

1250   That there could be unexplained variance with a data set that reports the three values of mass,
1251   BMR and length for individual animals is suspected because MMLE theory as currently
1252   expressed does not account for body temperature effects on the mitochondrion capability
1253   quotient. Body temperature has a significant effect on BMR (Clarke, Rothery & Isaac, 2010;
1254   Kolokotrones et al, 2010). The extent to which the inclusion of temperature effects on the
1255   mitochondrion capability quotient would improve MMLE's accuracy awaits a complete data set
1256   reporting body temperature as well as mass, BMR and length for individual animals. In the
1257   meantime, the body temperature data in (Kolokotrones et al, 2010) could be used to examine the
1258   extent to which inclusion of temperature in equation (3) would narrow the sturdiness factor range
1259   needed to bound the (Kolokotrones et al, 2010) BMR and mass data and the (Nowak, 1999) mass
1260   and length data.

1261   Ten parameters were theoretically derived to predict BMR and body mass with MMLE. The
1262   skeletal muscle mass constant, G_m and the non-skeletal muscle mass constant, G_o should have
1263   the same values for all placental mammals. The non-skeletal muscle mass exponent, y with its
1264   associated dimensionality factor m, used in equation (3) to predict body mass may have at least
1265   two values although the results predicted with the two values are nearly indistinguishable for the
1266   group of animals to which they may apply: runners/walkers . The type of similarity applicable to
1267   an animal's skeletal muscles determines the values for the dynamic similarity constant, k, the
1268   fundamental propulsion frequency constant, c, and the fundamental propulsion frequency
1269   exponent, r, used in equation (3). The mitochondrion capability quotient, e, used in equation (3)
1270   should have the same approximate value for all animals with the same body temperature in the
1271   same phylogenetic group. Whether an animal is a ruminant Artiodactyl or not determines which
1272   value of the resting metabolic rate constant, G_r, to use in equation (2) to predict BMR. Finally,
1273   the characteristic length, l, and the sturdiness factor, s, for an individual animal is used in
1274   equations (2) and (3) to predict that animal's BMR and body mass. If the characteristic length is
1275   not available then an eleventh parameter, a scaling fraction, can be used to translate the available
1276   length datum into the characteristic length.

1277   The results of regression analyses were used to estimate numerical values for the parameters.
1278   Phylogenetic informed (PI) regression analysis was performed on taxon-averaged data using
1279   BayesTraits. AVG regression analysis was performed on individual body mass, characteristic
1280   length data. AVG regression is unique to MMLE theory. Parameter numerical values estimated
1281   from results obtained with the two regression techniques did differ. Commenting on which
1282   regression technique is superior was not a purpose of the present paper. In terms of the two
1283   MMLE measures of effectiveness, R_M^2 and R, body masses predicted by equation (3) and BMR
1284   predicted by equation (2) are nearly indistinguishable when using parameters estimated from the
1285   results of either technique.

The results of the regression analyses were also used to partition populations into animals that conform to geometric similarity and animals that do not. Geometric similarity implies that body mass scales as the cube of characteristic length and BMR scales as body mass raised to the 2/3 power. The body mass of animals that do not conform to geometric similarity scale with characteristic length raised to a power less than three and BMR scales with body mass raised to a power greater than 2/3. Thus the BMR of a mixture of species can appear to scale with body mass raised to a power greater than 2/3 as observed in 1960 by Hemmingsen as cited in (Hulbert & Else, 2004).

As noted in the summary of MMLE theory, ten or eleven parameters is not such a large number of parameters to predict the absolute values of an individual placental mammal's BMR and body mass. Except for the characteristic length scaling fraction, the parameters emerged from the theoretical derivation of MMLE from the principles of physics and physiology that were being considered. The reconciliation of Cricetidae with the rest of Rodentia, the reconciliation of Mustelidae with the rest of Carnivora or the division of bats into three new groups could appear to be forcing MMLE to fit the data. However these instances are legitimate uses of the degrees of freedom available with MMLE to explain differences that were observed in the data.

The values for the constants G_m, G_o and G_r were derived from running/walking placental mammal data. Since the values obtained in the present paper differ from the values obtained with the data that was available over a quarter of a century ago, it would not be surprising if the values should be refined again in the future.

MMLE represents the vertebrate body as being composed of two types of tissues: volume active tissues in which mitochondria are approximately uniformly distributed; and surface active tissues in which the mitochondria are concentrated in surfaces that surround material with few mitochondria. The volume active tissues are associated with the skeletal musculature whose morphology is governed by dynamic similarity. The surface active tissues are associated with liver, heart, kidneys, and brain which is better represented as geometrically similar for Rodentia and Bats. For the mass of running/walking Artiodactyla and Carnivora predicted by equation (3) a geometrically similar representation in which surface area scales as volume raised to the 2/3 power is nearly indistinguishable from a topology in which surface area scales as volume raised to the 4/5 power.

 Using equation (3) the ratio of volume active tissue mass to total body mass for geometrically similar running/walking placental mammals is calculated to vary form 81% for sturdy animals to 93% for gracile animals. For Strouhal-Froude dynamically similar animals the ratio varies from 87% for small sturdy animals to 91% for small gracile animals; and for large animals it varies from 61% for sturdy animals to 74% for gracile animals. The ratio of muscle to total body mass appears to vary between 21% and 61% for mammals (Muchlinski, Snodgrass & Terranova, 2012). The MMLE volume active tissues appear to be about twice as massive as the skeletal musculature. This leads to the possibility that inclusion of a third type of tissue in the MMLE

1324 representation of the vertebrate body may be warranted. The third tissue type would include
1325 everything that is not skeletal muscle, liver, heart, kidneys, and brain. It would have few
1326 mitochondria so that it would contribute little to BMR.

1327 Three types of dynamic similarity were encountered for the skeletal musculature of the placental
1328 mammals examined in the present paper: Froude similarity, Strouhal similarity and simultaneous
1329 Froude and Strouhal similarity. Geometric similarity is compatible with either Froude or
1330 Strouhal similarity. It is not compatible with simultaneous Froude and Strouhal similarity. The
1331 type of dynamic similarity that governs the morphology of an animal's skeletal musculature
1332 seems to correlate with a phylogenetic level that may be as low as the species.

1333 Compared with the original paper (Frasier, 1984), the present paper makes important
1334 modifications to MMLE theory. The fundamental propulsion frequency is generalized to $f = c/l^r$
1335 where c is the fundamental propulsion frequency constant, l is the characteristic length and r is
1336 the fundamental propulsion frequency exponent. This generalization allows the different types of
1337 dynamic similarity to be explicitly addressed by equation (3). The mass of the non-skeletal
1338 musculature is also generalized to allow non-geometrically similar topologies to be explicitly
1339 addressed by equation (3). Ordinary Least Squares regression analyses are replaced by PI
1340 analyses in the present paper. The present paper estimates new numerical values for the
1341 parameters occurring in equations (2) and (3) by analysis of data that was unavailable when the
1342 original paper was written. The present paper furthermore extends the demonstration of MMLE
1343 theory's ability to exactly predict body mass and BMR for individual animals from about 9% of
1344 placental mammals to about 72% by adding Rodentia and bats to running/walking Artiodactyla,
1345 Carnivora, Perissodactyla and Proboscidae.

1346 Carnivora with body masses less than about 2000g were not included in the body mass as a
1347 function of characteristic length analysis of running/walking placental mammals. They were not
1348 included because their shoulder heights are not given in (Nowak, 1999). However head and body
1349 lengths are given. The methodology of using a scaling fraction to translate heady and body
1350 length to characteristic length as was done for Rodentia may also work for small Carnivora.

1351 MMLE's ability to predict BMR and body mass for the mammal orders that were not included in
1352 the present paper should be examined. A complication is that from an examination of
1353 (Kolokotrones et al, 2010) it appears that BMR data are scarce except for the orders Primates,
1354 Soricomorpha, Dasyuromorpha and Diprotodontia.

1355 MMLE should apply to all vertebrates. The original paper tried to address birds but that analysis
1356 now appears to be simplistic. The analysis should be performed again with recent data and the
1357 expanded version of MMLE presented in the present paper.

1358 The examination of body mass and BMR from the skeletal length perspective rather than from
1359 the body mass perspective lead to the concept of the sturdiness factor in MMLE theory. The
1360 sturdiness factor adds additional information about the composition of an animal's body that is

1361 missing from relationships of the form aW^b. Consideration of body composition can reduce
1362 unexplained variance even for relationships that express BMR as a function of body mass
1363 (Raichlen et al, 2010; Müller et al, 2011). MMLE explains all the variance for an animal's BMR
1364 and body mass. Compared to the variance explained by the PI regression relationships of the
1365 form BMR = aW^b in tables 1, 2 and 3, MMLE explains an additional 2.5% to 18.5% of the
1366 variance. The sturdiness factor is a major contributor to this additional explained variance.

1367 The (Raichlen, Pontzer & Shapiro, 2013) finding that hip joint to limb center of mass length is a
1368 better length for establishing the pendulum frequency for Froude-Strouhal similar animals may
1369 affect the concept of the sturdiness factor. Sturdier animals have stouter limbs which should
1370 cause the limb's center of mass to be further from the hip joint and thereby increase the
1371 characteristic length. For this reason it is possible that the sturdiness factor may be, in part, a
1372 scaling factor for converting characteristic length surrogates such as shoulder height into hip
1373 joint to limb center of mass lengths.

1374 While the mitochondrion capability quotient used in equation (3) should have approximately the
1375 same value for all animals with the same body temperature in the same phylogenetic group,
1376 genetic variation could cause it to vary among individuals or populations in the same species.
1377 Variation of the mitochondrion capability coefficient together with variation of the sturdiness
1378 factor would cause mass-independent variation in the BMR of animals like that recently
1379 addressed by White and Kearney (White & Kearney, 2013).

1380 MMLE was derived for fit animals surviving in the wild. Captivity, domestication, inactivity and
1381 sickness could cause an animal's body mass or BMR to be different from that predicted by
1382 MMLE. In particular, muscle or mitochondrion atrophy due to decreased activity with respect to
1383 that experienced in the wild would likely cause a difference.

1384 **Conclusion.** The purpose of this paper was to use modern resources to revisit MMLE theory and
1385 test its ability to predict the absolute values of BMR and body mass for individual animals. With
1386 some modifications to the theory as originally formulated (Frasier, 1984) MMLE can exactly
1387 predict every individual BMR given body mass datum and every individual body mass given
1388 characteristic length datum for the recent data sets that were examined (Nowak, 1999;
1389 Kolokotrones et al, 2010) and for the mammal orders examined. MMLE deterministically
1390 predicts the absolute value of BMR and body mass for individual animals rather than a statistical
1391 best fit average value for a collection of individuals from a single species which is the usual
1392 methodology used by other examinations of these topics (White & Kearny, 2014). With MMLE
1393 there is no error and thus no unexplained variance. The examined mammal orders include over
1394 two thirds of recent mammal species.

1395 Determining if MMLE can simultaneously exactly predict an individual animal's BMR and body
1396 mass given its characteristic length awaits a data set that simultaneously reports all three values
1397 for individual animals. However MMLE's ability to predict the BMR regressed on mass

exponent obtained by PI regression analysis of the (Kolokotrones et al, 2010) BMR and mass data from the mass regressed on length exponent obtained by AVG regression analysis of the (Nowak, 1999) length and mass data for many of the MMLE phylogenetic homogeneous groups addressed in this paper argues that accurate simultaneous prediction of mass and BMR for the same animal may be possible.

Supplemental Information.

Data S1.

Running-walking placental mammals masses and shoulder heights.

Data S2.

Rodentia masses and lengths.

Data S3.

Chiroptera (Bats) masses and lengths.

Article S1.

Methods Details.

References.

Agutter PS, Tuszynski JA. 2011. Analytic theories of allometric scaling. *The journal of experimental biology* 214: 1055-62.

Alexander RM, Jayes AS, Malioy GM, Wathuta EM. 1979. Allometry of the limb bones of mammals from shrews Sorex. to elephant Loxodonta.. *Journal of zoology : proceedings of the Zoological Society of London* 189: 305-314.

Alexander RM. 2005. Models and the scaling of energy costs for locomotion. *The journal of experimental biology* 208: 1645-52.

Banavar JR, Moses ME, Brown JH, Damuth J, Rinaldo A, Sibly RM, Maritan A. 2010. A general basis for quarter-power scaling in animals. *Proceedings of the National Academy of Sciences of the United States of America* 107: 15816-20.

Biewener AA. 2005. Biomechanical consequences of scaling. *The journal of experimental biology* 208: 1665-76.

Bullen RD, McKenzie NL. 2002. Scaling bat wingbeat frequency and amplitude. *The journal of experimental biology* 205: 2615-26.

Campione NE, Evans DC. 2013. A universal scaling relationship between body mass and proximal limb bone dimensions in quadrupedal terrestrial tetrapods. *BMC biology* 10:60.

Capellini I, Venditti C, Barton RA. 2010. Phylogeny and metabolic scaling in mammals. *Ecology* 91: 2783-93.

Christiansen P. 1999. Scaling of the limb long bones to body mass in terrestrial mammals. *Journal of Morphology* 239: 167-90.

Clarke A, Rothery P, Isaac NJ 2010. Scaling of basal metabolic rate with body mass and temperature in mammals. *The Journal of animal ecology* 79: 610-9.

da Fonseca RR, Johnson WE, O'Brien SJ, Ramos MJ, Antunes A. 2010. The adaptive evolution of the mammalian mitochondrial genome. *BMC Genomics* 9: 119.

Economos AC. 1982. On the origin of biological similarity. *Journal of theoretical biology* 94: 25-60.

Edwards AL. 1984. *An introduction to linear regression and correlation*. New York: W. H. Freeman. 32 .

Else PL, Hulbert AJ. 1981. Comparison of the "mammal machine" and the "reptile machine": energy production. *The American journal of physiology* 240: R3-R9.

1448 Else PL, Hulbert AJ. 1985. An allometric comparison of the mitochondria of mammalian and
1449 reptilian tissues: the implications for the evolution of endothermy. *Journal of comparative*
1450 *physiology. B, Biochemical, systemic, and environmental physiology* 156: 3-11.

1451 Frasier CC. 1984. An explanation of the relationships between mass, metabolic rate and
1452 characteristic length for birds and mammals. *Journal of theoretical biology* 109: 331-371.

1453 Freckleton RP, Harvey PH, Pagel M. 2002. Phylogenetic analysis and comparative data: a test
1454 and review of evidence. *The American naturalist* 160: 712-26.

1455 Fritz SA, Bininda-Emonds OR, Purvis A. 2009. Geographical variation in predictors of
1456 mammalian extinction risk: big is bad, but only in the tropics. *Ecology letters* 2009 12: 538-49.

1457 Garcia GJ, da Silva JK. 2004. On the scaling of mammalian long bones. *The journal of*
1458 *experimental biology* 207: 1577-84.

1459 Glazier DS. 2010. A unifying explanation for diverse metabolic scaling in animals and plants.
1460 *Biological reviews of the Cambridge Philosophical Society* 85: 111-38.

1461 Guderley H, Turner N, Else PL, Hulbert AJ. 2005. Why are some mitochondria more powerful
1462 than others: insights from comparisons of muscle mitochondria from three terrestrial vertebrates.
1463 *Comparative biochemistry and physiology. Part B, Biochemistry & molecular biology* 142: 172-
1464 80.

1465 Hudson LN, Isaac NJ, Reuman DC. 2013. The relationship between body mass and field
1466 metabolic rate among individual birds and mammals. *The journal of animal ecology* 82: 1009-
1467 20.

1468 Hulbert AJ, Else PL 1999. Membranes as possible pacemakers of metabolism. *Journal of*
1469 *theoretical biology* 199: 257-74.

1470 Hulbert AJ, Else PL. 2004. Basal metabolic rate: history, composition, regulation, and
1471 usefulness. *Physiological and biochemical zoology* 77: 869-76.

1472 Iriarte-Diaz J, Riskin DK, Breuer KS, Swartz SM. 2012. Kinematic plasticity during flight in
1473 fruit bats: individual variability in response to loading. *PLoS One.* 7(5): e36665.

1474 Isaac NJ, Carbone C. 2010. Why are metabolic scaling exponents so controversial? Quantifying
1475 variance and testing hypotheses. *Ecology letters* 13: 728-35.

1476 Jastroch M, Divakaruni AS, Mookerjee S, Treberg JR, Brand MD. 2010. Mitochondrial proton
1477 and electron leaks. *Essays in biochemistry* 47: 53-67.

1478 Kleiber M. 1932. Body size and metabolism. *Hilgardia* 6: 315-353.

1479 Kleiber M. 1961. The fire of life: *An introduction to animal energetics*. New York: John Wiley
1480 & Sons.

1481 Kolokotrones T, Savage V, Deeds E.J, Fontana, W. 2010. Curvature in metabolic scaling.
1482 *Nature* 464: 753-756.

1483 Kozlowski J, Konarzewski M, Gawelczyk AT. 2003. Cell size as a link between noncoding DNA
1484 and metabolic rate scaling. *Proceedings of the National Academy of Sciences of the United*
1485 *States of America* 100: 14080-5.

1486 Maino JL, Kearney MR, Nisbet RM, Kooijman SA. 2014. Reconciling theories for metabolic
1487 scaling. The Journal of animal ecology 83: 20-29.

1488 McMahon TA. 1973. Size and shape in biology. *Science* 179: 1201-1204.

1489 McMahon TA. 1975. Allometry and biomechanics: limb bones in adult ungulates. *The American*
1490 *naturalist* 109: 547-563.

1491 McNab BK. 1988. Complications inherent in scaling the basal rate of metabolism in mammals.
1492 *The Quarterly review of biology* 63: 25-54.

1493 McNab, BK. 1997. On the utility of uniformity in the definition of basal rate of metabolism.
1494 *Physiological zoology* 70: 718–720

1495 McNab BK. 2008. An analysis of the factors that influence the level and scaling of mammalian
1496 BMR. *Comparative biochemistry and physiology. Part A, Molecular & integrative physiology*
1497 151: 5-28.

1498 Muchlinski MN, Snodgrass JJ, Terranova CJ. 2012. Muscle mass scaling in primates: an
1499 energetic and ecological perspective. *American journal of primatology* 74: 395-407.

1500 Muijres FT, Johansson LC, Winter Y, Hedenström A. 2011. Comparative aerodynamic
1501 performance of flapping flight in two bat species using time-resolved wake visualization.
1502 *Journal of the Royal Society, Interface / the Royal Society* 8: 1418-28.

1503 Müller MJ, Langemann D, Gehrke I, Later W, Heller M, Glüer CC, Heymsfield SB, Bosy-
1504 Westphal A. 2011. Effect of constitution on mass of individual organs and their association with
1505 metabolic rate in humans--a detailed view on allometric scaling. *PLoS One*. 6(7): e22732.

1506 Müller MJ, Wang Z, Heymsfield SB, Schautz B, Bosy-Westphal A. 2013. Advances in the
1507 understanding of specific metabolic rates of major organs and tissues in humans. *Current opinion*
1508 *in clinical nutrition metabolic care.* 16: 501-8.

1509   Norberg UM. 1981. Allometry of Bat Wings and Legs and Comparison with Bird Wings.
1510   *Philosophical transactions of the Royal Society of London. Series B, Biological sciences* 292:
1511   359-398.

1512   Norberg, UM, Rayner, JMV. 1987. Ecological morphology and flight in bats Mammalia;
1513   Chiroptera.: wing adaptations, flight performance, foraging strategy and echolocation.
1514   *Philosophical transactions of the Royal Society of London. Series B, Biological sciences* 316:
1515   335–427.

1516   Norberg UM, Norberg RA. 2012. Scaling of wingbeat frequency with body mass in bats and
1517   limits to maximum bat size. *The journal of experimental biology* 215: 711-22.

1518   Nowak RM. 1999. *Walker's mammals of the world*. Baltimore: John Hopkins.

1519   Nudds RL, Taylor GK, Thomas AL. 2004. Tuning of Strouhal number for high propulsive
1520   efficiency accurately predicts how wingbeat frequency and stroke amplitude relate and scale with
1521   size and flight speed in birds. *Proceedings. Biological sciences / The Royal Society* 271: 2071-6.

1522   Nyakatura K, Bininda-Emonds OR. 2013. Updating the evolutionary history of Carnivora
1523   Mammalia.: a new species-level supertree complete with divergence time estimates. *BMC*
1524   *Biology* 10: 12.

1525   Pagel M. 1999. Inferring the historical patterns of biological evolution. Nature. 401: 877-84.

1526   Pagel M, Meade A, Barker D. 2004. Bayesian estimation of ancestral character states on
1527   phylogenies. *Systematic Biolology* 2004 53: 673-84.

1528   Raichlen DA, Gordon AD, Muchlinski MN, Snodgrass JJ. 2010. Causes and significance of
1529   variation in mammalian basal metabolism. *Journal of comparative physiology. B, Biochemical,*
1530   *systemic, and environmental physiology* 180: 301-11.

1531   Raichlen DA, Pontzer H, Shapiro LJ. 2013. A new look at the dynamic similarity hypothesis: the
1532   importance of the swing phase. *Biology open* 19: 1032-6

1533   Riskin DK, Iriarte-Díaz J, Middleton KM, Breuer KS, Swartz SM. 2010. The effect of body size
1534   on the wing movements of pteropodid bats, with insights into thrust and lift production. J *The*
1535   *journal of experimental biology* 213: 4110-22.

1536   Roberts MF, Lightfoot EN, Porter WP. 2010. A new model for the body size-metabolism
1537   relationship. *Physiological and biochemical zoology* 83: 395-405.

1538   Roberts MF, Lightfoot EN, Porter WP. 2011. Basal metabolic rate of endotherms can be
1539   modeled using heat-transfer principles and physiological concepts: reply to "can the basal
1540   metabolic rate of endotherms be explained by biophysical modeling?". *Physiological and*
1541   *biochemical zoology* 84: 111-4.

1542 Savage VM, Gillooly JF, Woodruff WH, West GB, Allen AP, et al. 2004. The predominance of
1543 quarter-power scaling in biology. *Functional Ecology* 18: 257-282.

1544 Seebacher F, Brand MD, Else PL, Guderley H, Hulbert AJ, Moyes CD. 2010. Plasticity of
1545 oxidative metabolism in variable climates: molecular mechanisms. *Physiological and*
1546 *biochemical zoology : PBZ* 83: 721-32.

1547 Seymour RS, White CR. 2011. Can the basal metabolic rate of endotherms be explained by
1548 biophysical modeling? Response to "a new model for the body size-metabolism relationship".
1549 *Physiological and biochemical zoology* 84: 107-10.

1550 Smith, R.E. 1956. Quantitative relations between liver mitochondria metabolism and total body
1551 weight in mammals. *Annals of the New York Academy of Sciences* 62: 403-421.

1552 Sousa T, Domingos T, Poggiale JC, Kooijman SA. 2010. Dynamic energy budget theory restores
1553 coherence in biology. *Philosophical transactions of the Royal Society of London. Series B,*
1554 *Biological sciences* 365: 3413-28.

1555 Taylor GK, Nudds RL, Thomas AL. 2003. Flying and swimming animals cruise at a Strouhal
1556 number tuned for high power efficiency. *Nature* 425: 707-11.

1557 Walker EP. 1968. *Mammals of the World*. Baltimore. John Hopkins.

1558 Wang Z, O'Connor TP, Heshka S, Heymsfield SB. 2001. The reconstruction of Kleiber's law at
1559 the organ-tissue level. *The Journal of nutrition* 131: 2967-70.

1560 West GB, Brown JH, Enquist BJ. 1997. A general model for the origin of allometric scaling laws
1561 in biology. *Science* 276: 122-126.

1562 White CR, Seymour RS. 2003. Mammalian basal metabolic rate is proportional to body mass2/3.
1563 *Proceedings of the National Academy of Sciences of the United States of* America 100: 4046-9.

1564 White CR, Blackburn TM, Seymour RS. 2009. Phylogenetically informed analysis of the
1565 allometry of Mammalian Basal metabolic rate supports neither geometric nor quarter-power
1566 scaling. *Evolution; international journal of organic evolution* 63: 2658-67.

1567 White, C.R. There is no single p. 2010. Nature 464: 691.

1568 White CR, Kearney MR, Matthews PG, Kooijman SA, Marshall DJ. 2011. A manipulative test
1569 of competing theories for metabolic scaling. *The American naturalist* 178: 746-54.

1570 White CR, Frappell PB, Chown SL. 2012. An information-theoretic approach to evaluating the
1571 size and temperature dependence of metabolic rate. *Proceedings. Biological sciences / The*
1572 *Royal Society* 279: 3616-21

1573   White CR, Kearney MR. 2013. Determinants of inter-specific variation in basal metabolic rate.
1574   *Journal of comparative physiology. B, Biochemical, systemic, and environmental physiology*
1575   183: 1-26

1576   White CR, Kearney MR. 2014. Metabolic scaling in animals: methods, empirical results, and
1577   theoretical explanations. *Comprehensive Physiology* 4: 231-56

1578